
Doctoral Dissertations

Student Theses and Dissertations

1978

Adaptive control of a cloud simulation chamber expansion system

Katiya Greigarn

Follow this and additional works at: https://scholarsmine.mst.edu/doctoral_dissertations



Part of the [Electrical and Computer Engineering Commons](#)

Department: **Electrical and Computer Engineering**

Recommended Citation

Greigarn, Katiya, "Adaptive control of a cloud simulation chamber expansion system" (1978). *Doctoral Dissertations*. 341.

https://scholarsmine.mst.edu/doctoral_dissertations/341

This thesis is brought to you by Scholars' Mine, a service of the Missouri S&T Library and Learning Resources. This work is protected by U. S. Copyright Law. Unauthorized use including reproduction for redistribution requires the permission of the copyright holder. For more information, please contact scholarsmine@mst.edu.

ADAPTIVE CONTROL OF A CLOUD SIMULATION
CHAMBER EXPANSION SYSTEM

BY

KATIYA GREIGARN, 1952-

A DISSERTATION

Presented to the Faculty of the Graduate School of the

UNIVERSITY OF MISSOURI-ROLLA

In Partial Fulfillment of the Requirements for the Degree


DOCTOR OF PHILOSOPHY

T4386


in c. 1
87 pages

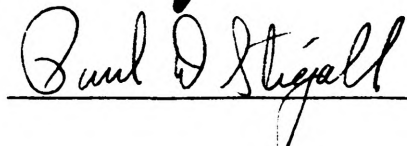
ELECTRICAL ENGINEERING

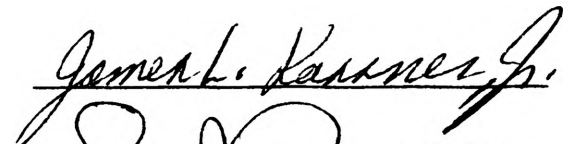
1978



Advisor











ABSTRACT

This dissertation describes the design and construction of a closed-loop computer controlled expansion system for a cloud simulation chamber. The chamber is used to simulate atmospheric phenomena for the study of microphysical processes. In order to accomplish this, the sample gas inside the chamber must be expanded adiabatically. This means the wall temperature and the gas temperature must be made to agree as closely as possible. The wall is cooled by thermoelectric modules, and the temperature is controlled by analog controllers. The gas is cooled by the adiabatic expansion, and the corresponding pressure is controlled by a laboratory minicomputer, a NOVA 840. The range of operation of the expansion system is specified to be 20.7 kPa (3 psi) change in pressure. The accuracy and the rms error must be better than ± 0.0207 kPa (± 0.003 psi) and 0.0414 kPa (0.006 psi), respectively. This range of operation is large enough that an analog controller can not obtain an adequate result. The error arises due to the fact that the input function is a ramp and the expansion system has multiple non-linearities.

In order to obtain zero steady state error, the time-optimal control is implemented by the minicomputer. Table look-up and on-line identification schemes for the system parameters have been investigated. An adaptive control algorithm using on-line identification outperforms the table look-up method due the flexibility of the identification

scheme. Special efforts are made to adjust the identification scheme so that the model parameters converge close to the system parameters within one step. The results indicate that the closed-loop computer controlled expansion system yields the desired specification.

ACKNOWLEDGEMENT

The research described herein was conceived by Dr. James L. Kassner, Jr. for use with the Cloud Simulation System. Due to the size of the problems, many people and ideas were involved. The author would like to thank Dr. Daniel R. White, David C. Hollocher and Alfred R. Hopkins for their technical support during the installation of the system design.

The author also appreciates the assistance given by Dr. Donald E. Hagen and Dr. Kui C. Lam for their computer programming discussion. The author gratefully acknowledges Dr. K. R. Dunipace and his advisor, Dr. D. R. Fannin, for having suggested the dissertation topic and for valuable guidance throughout the course of this work. Acknowledgements are also extended to Dr. Frank J. Kern, Professor Sylvester J. Pagano, Dr. Paul D. Stigall, Dr. James L. Kassner, Jr. and Dr. Earl F. Richards for serving on the committee.

The author wishes to thank his parents, his aunt, Dr. Sumana Greigarn, and his fiancée, Poonsamon Sritalapat for their continued encouragement during his studies. And thanks go to Leah Pagel for typing this dissertation.

All the work was supported by the Cloud Physics Research Center and NASA, Grant Number NAS8-31849.

TABLE OF CONTENTS

	Page
ABSTRACT	ii
ACKNOWLEDGEMENT.	iv
LIST OF ILLUSTRATIONS	vii
LIST OF TABLES	x
I. INTRODUCTION	1
II. REVIEW OF THE LITERATURE ON CLOUD SIMULATION CHAMBERS	9
III. DIRECT DIGITAL CONTROL SYSTEM DESIGN	13
A. DESIGN SPECIFICATION	13
B. EXPANSION CONTROL SYSTEM HARDWARE	14
1. The Cloud Simulation Chamber.	14
2. The Positive Displacement Uni-Directional Pump.	14
3. The Regulator Tank.	15
4. The Storage Tank.	15
5. The 3-Way Infinite Position Rotary Valve.	15
6. The Solenoid and Manual Valves.	16
7. The Pressure Gauge.	16
8. The Pressure Relief Valve	16
9. The Stepping Motor and Stepping Motor Interface.	17
10. The Transducers	19
11. The Computer System	23

TABLE OF CONTENTS (cont.)

	Page
C. MODEL OF THE EXPANSION SYSTEM	23
D. SYSTEM SOFTWARE	28
1. The Implementation of the Time-Optimal Control.	28
2. The Implementation of the Adaptive Control Algorithm.	34
3. System Programming	41
IV. EXPERIMENTAL RESULTS	48
V. CONCLUSION.	70
BIBLIOGRAPHY	73
VITA	78

LIST OF ILLUSTRATIONS

Figure	Page
1.1. The layout of the expansion system.	6
1.2. The block diagram of the computer controlled expansion system	8
3.1. The number format of the stepping motor interface	18
3.2. The flow chart of the stepping motor interface output routine.	20
3.3. The NOVA 840 computer system.	22
3.4. The electrical analogy of the expansion system.	25
3.5. Block diagram of the closed-loop digital control of the expansion system.	30
3.6. The implementation of the time-optimal control algorithm	32
3.7. The sequential regression identification subroutine.	37
3.8. The behavior of the coefficient A as a function of time. The rate of expansion is $-4^{\circ}\text{C}/\text{min}$	39
3.9. The behavior of the coefficient B as a function of time. The rate of expansion is $-4^{\circ}\text{C}/\text{min}$	40
3.10. The block diagram of overall identification scheme	42
3.11. The flow chart of the subroutine PREPAR . . .	45
3.12. The flow chart of PRESC	46
4.1. The coefficient A when A and B are initially set at 0.5 and 0.03, respectively .	49
4.2. The coefficient B when A and B are initially set at 0.5 and 0.03, respectively.	50

LIST OF ILLUSTRATIONS (cont.)

Figure	Page
4.3. The error of the pressure response when A and B are initially set at 0.5 and 0.03, respectively	51
4.4. The pressure response when being recorded every 2 seconds	53
4.5. The pressure error when being recorded every 2 seconds.	54
4.6. The pressure response at the rate of expansion of -0.1242 kPa/s or $-6^{\circ}\text{C}/\text{min}$	55
4.7. The pressure error at the rate of expansion of -0.1242 kPa/s or $-6^{\circ}\text{C}/\text{min}$	56
4.8. The coefficient A at the expansion rate of -0.1242 kPa/s or $-6^{\circ}\text{C}/\text{min}$	57
4.9. The coefficient B at the expansion rate of -0.1242 kPa/s or $-6^{\circ}\text{C}/\text{min}$	58
4.10. The pressure response at the expansion rate of -0.0828 kPa/s or $-4^{\circ}\text{C}/\text{min}$	59
4.11. The pressure error at the expansion rate of -0.0828 kPa/s or $-4^{\circ}\text{C}/\text{min}$	60
4.12. The coefficient A at the expansion rate of -0.0828 kPa/s or $-4^{\circ}\text{C}/\text{min}$	61
4.13. The coefficient B at the expansion rate of -0.0828 kPa/s or $-4^{\circ}\text{C}/\text{min}$	62
4.14. The pressure response at the expansion rate of -0.0414 kPa/s or $-2^{\circ}\text{C}/\text{min}$	63
4.15. The pressure error at the expansion rate of -0.0414 kPa/s or $-2^{\circ}\text{C}/\text{min}$	64
4.16. The coefficient A at the expansion rate of -0.0414 kPa/s or $-2^{\circ}\text{C}/\text{min}$	65
4.17. The coefficient B at the expansion rate of -0.0414 kPa/s or $-2^{\circ}\text{C}/\text{min}$	66

LIST OF ILLUSTRATIONS (cont.)

Figure		Page
4.18.	The pressure response including the holding modes	67
4.19.	The pressure error including the holding modes	68

LIST OF TABLES

Table		Page
I	Typical Table Look-up Model of the Expansion System	33
II	Experimental Values of AFILTER and BFILTER . .	43

I. INTRODUCTION

For centuries, man has observed and studied the weather phenomena of the atmosphere. It has been demonstrated that delicate microphysical processes occurring in the atmosphere have a large influence on the amount and character of precipitation. As technology has become more advanced, man has tried to develop a tool to control his environment in order to protect himself from inadequate precipitation and from polluted atmosphere. An invariably successful process for producing rain and snow would have tremendous significance for virtually everyone. Hence, recent experiments in the production of man-made precipitation have aroused wide interest [1-4].

At present, it is commonly known that the atmosphere contains a large quantity of solid and liquid particles. The majority of these particles are concentration nuclei, which appear at different supersaturations. The total concentration of atmospheric condensation nuclei (Aitken nuclei) is determined by counters in which moist air is cooled during adiabatic expansion [5-6]. The condensation nuclei play an important part in cloud formation. For example, if moist air is admitted into a chamber and expanded, cloud or fog will form in the chamber as a result of the cooling caused by the adiabatic expansion. The same air produces successively decreasing amounts of fog with successive expansions. If the air is made to pass

through a filter of packed cotton before entering the chamber, it is found that no cloud or fog forms. The decreasing amounts of cloud or fog formed during each repeated expansion suggest that the air becomes "exhausted" of nuclei. The lack of condensation when filtered air is expanded indicates that the nuclei operative in this case may be removed by means of a mechanical filter. The filtered air becomes again capable of producing cloud or fog if smoke is introduced into the chamber.

These microphysical processes may be carefully controlled and studied in the laboratory. In order to simulate real atmospheric conditions, a sample gas in the chamber must be expanded by an adiabatic process. Careful consideration must be given to the effects of heat flow from the wall of the chamber. This is due to the very large heat capacity of the wall in comparison to the heat capacity of the gas inside the chamber. In a laboratory environment, heat flow occurs between the chamber wall and the gas because the gas is cooler than the wall after the expansion begins. To eliminate the temperature gradient between the wall and the gas, they must be maintained at the same temperature at all times during the expansion. This may be accomplished by cooling the chamber walls and controlling the gas pressure and the wall temperature very precisely. Such a cloud simulation chamber and its supporting subsystems have been developed at the University of Missouri-Rolla. The chamber is made of aluminum. It is

a ten-sided right prism, 61 centimeters high and 48 centimeters in diameter. It has a volume of 0.11 cubic meters and 1.3 square meters inner wall surface. Subsystems are required to clean and humidify the sample gas and prepare an aerosol to provide nucleation sites of the cloud. For the wall cooling system, there are 836 thermoelectric modules sandwiched between the inner wall and the heat sink of the chamber. The thermoelectric module has the property that when electric current is passed through it the module can extract heat from the wall and pump it into the heat sink. The temperature of the heat sink is regulated by means of a circulating constant temperature bath. The inner wall temperature is monitored by transistor thermometers mounted in holes drilled through the back of the inner wall and extending to within 0.2 mm of the inside surface. These transistor thermometers are accurate to within a few millidegrees Celsius. The inner wall temperature is controlled by twenty-eight closed-loop analog controllers with a compensator in each loop and another compensator at the input [7]. The wall temperature has a small steady state offset, less than $10\text{ m}^{\circ}\text{C}$ per degree per minute of input ramp slope. The settling time is about one minute. The maximum cooling rate which can be closely controlled is $7^{\circ}\text{C}/\text{min}$. The absolute maximum cooling rate (power limited) is $10^{\circ}\text{C}/\text{min}$.

The gas temperature must also be controlled to follow the wall temperature, or, in other words, both the gas

temperature and the wall temperature must follow each other as closely as possible. Unfortunately, the temperature of the gas in a supersaturated system cannot be measured directly with fine wire thermocouples because the latent heat of condensation is liberated on the element, thus causing a displacement of the observed temperature. In addition, the surface condition of the measuring element affects the onset of condensation. However, the pressure of the gas can be directly measured. In conjunction with the initial pressure P_0 and the initial equilibrium temperature T_0 of the gas in the chamber, the gas temperature at any time during the simulation can be computed by the adiabatic gas law

$$\frac{T_1}{T_0} = \left(\frac{P_1}{P_0} \right)^{\frac{\gamma-1}{\gamma}} \quad (1.1)$$

where γ is the ratio of specific heat at constant pressure to the specific heat at constant volume for the same gas. The gas temperature at any time T_1 can be calculated from the measured value of pressure P_1 at that time. This equation can be applied only for a dry adiabatic expansion. The increase in gas temperature due to latent heat of vaporization given off by droplet condensation is neglected. In the cloud simulation experiment the effects of the latent heat can be corrected for if the liquid water content of the sample gas is known. Experimental techniques for measuring the liquid water content have been

developed. They are now being implemented [8]. Since corrections can be made for the effects of the latent heat, it is sufficient to test the performance of the wall temperature and pressure control systems under the conditions of a dry adiabatic expansion.

Due to the lack of a method for measuring the gas temperature directly, the expansion system uses the gas pressure as a variable for control purposes. The layout of the expansion system is shown in Figure 1.1. The cloud simulation chamber is considered as a closed container. The pressure inside the chamber can be governed by adjusting the orifice of the 3-way rotary valve, whose position is controlled by the step motor. The pressure is measured by a strain gauge type pressure transducer.

In analyzing the expansion control system, great care must be taken in assessing the importance of thermodynamic effects because they can introduce strong non-linearities into the system. The orifice is a series resistance which usually has a quadratic constitutive equation. For small perturbations in the flow, a linearized approximation can be used in the control design. For the expansion system, the linearized range of operation is relatively small in comparison to the total change of pressure which is 21 kPa (3 psi). The desired performance specifications cannot be met by a fixed, linear controller. Therefore, it is necessary to employ identification techniques and some

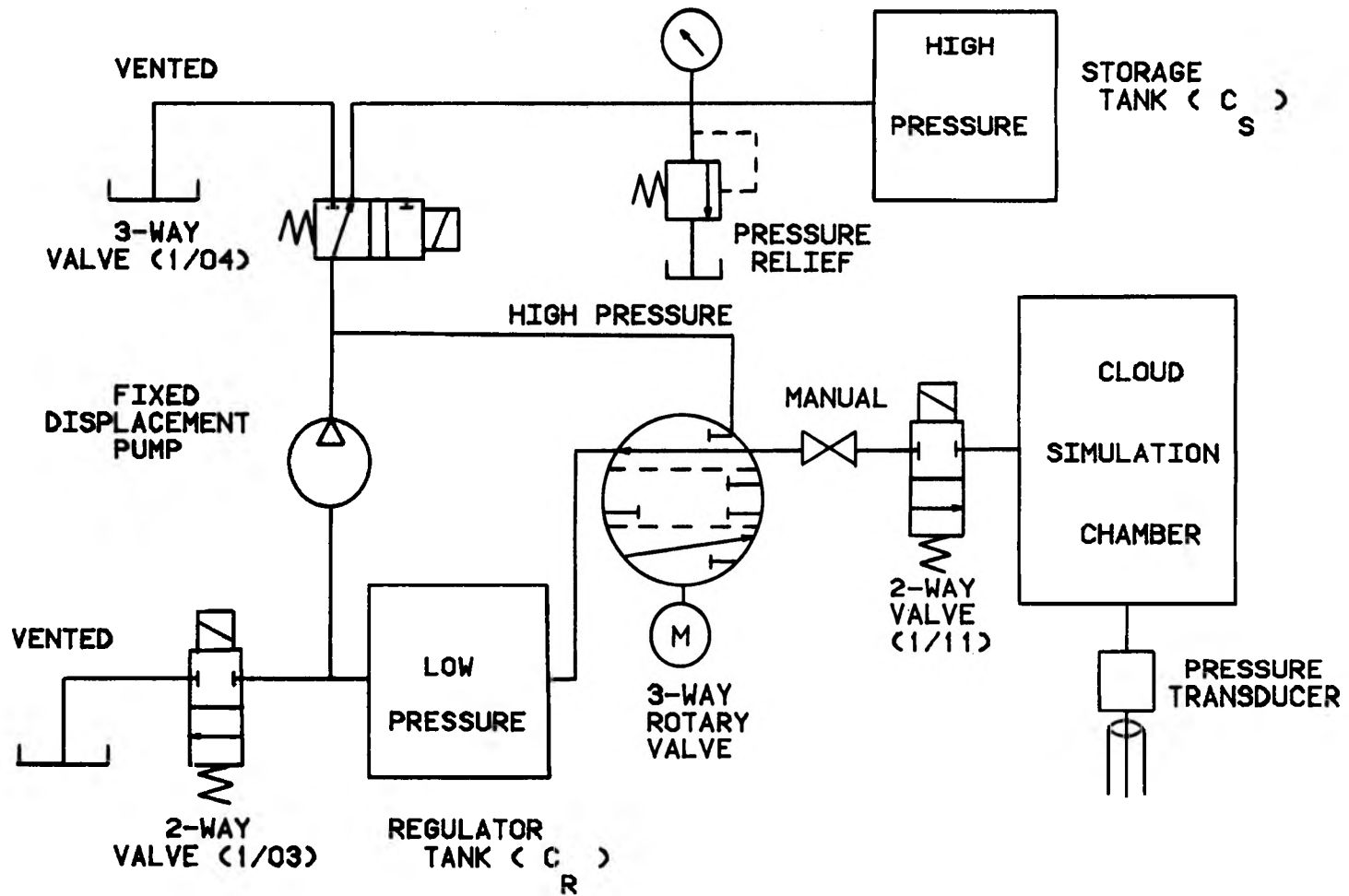


Figure 1.1. The layout of the expansion system

scheme of computing the control in real time. Such an identification and control scheme can realize the desired performance specifications. This dissertation describes the design and construction of the closed-loop, computer controlled expansion system using identification and real time computation of control. The block diagram is shown in Figure 1.2.

In a system such as that described above, the control law may be made to be optimum in some sense. Among the many different types of optimal control design problems, the time-optimal control and minimum integral square error are the most common. It can be shown that the optimal feedback gains obtained from the time-optimal control and minimum summed-square error control of the expansion system are the same [9-11]. As a consequence the time-optimal control is being used in the design because of its analytical simplicity.

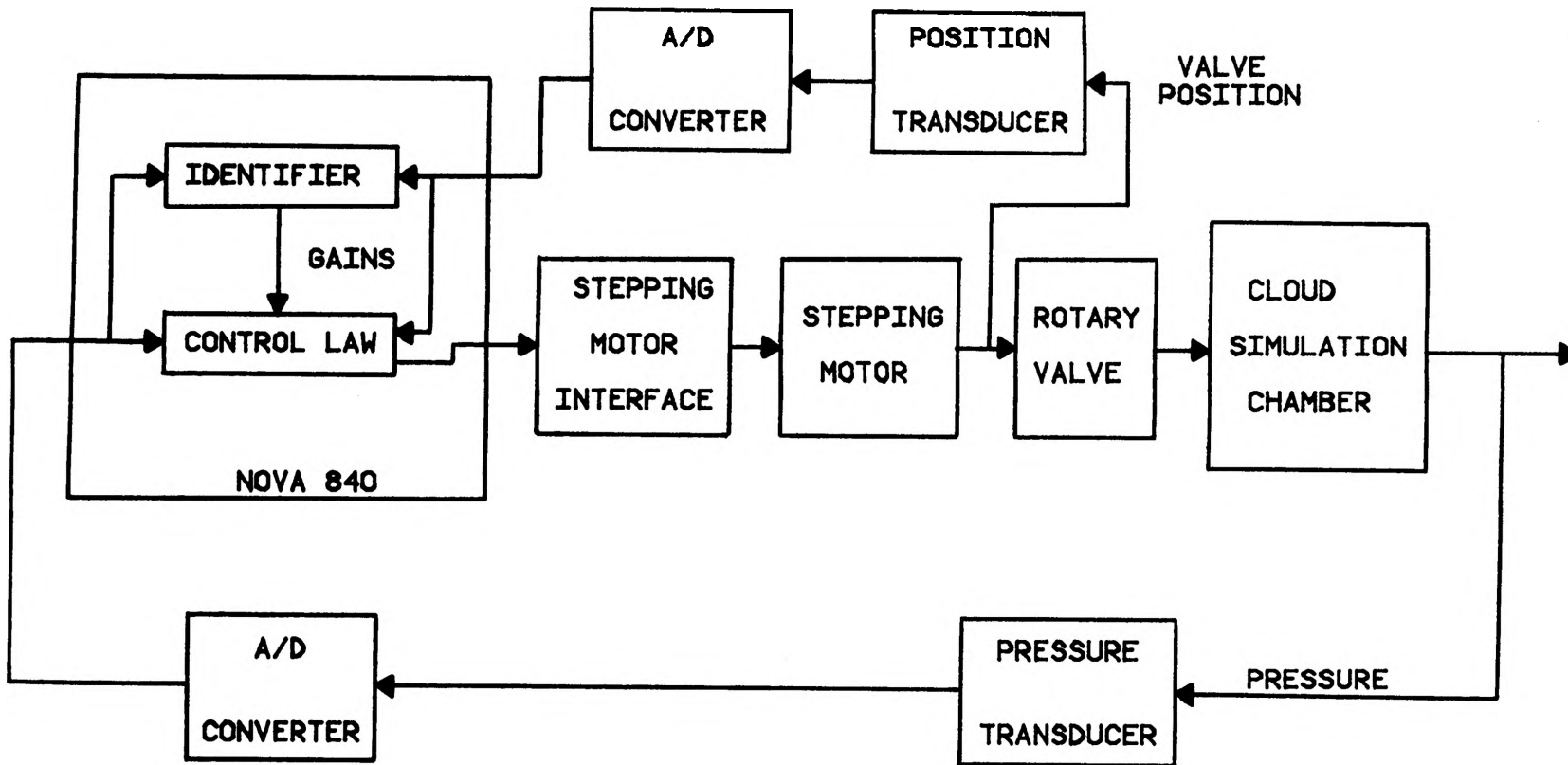


Figure 1.2. The block diagram of the computer controlled expansion system.

II. REVIEW OF THE LITERATURE ON CLOUD SIMULATION CHAMBERS

In the eighteenth century Kratzenstein resolved the question of whether cloud droplets are bubbles or liquid water spheres, using microscopic observations. This problem was later solved in a more systematic way by W. H. Dines [12] in 1880 and by R. Assmann in 1885. Simultaneously, the theory and measurement of condensation nuclei was developed. H. Beckquerel [6], in 1847, formulated with amazing clarity the existence and the physical role of condensation nuclei in atmospheric processes. M. Coulier [13] in 1875, and J. Aitken [5], in 1880, supported his ideas by observations and measurements.

Coulier enclosed air in a flask together with water and produced supersaturation by compressing a hollow india-rubber ball connected to the flask and then suddenly releasing it. In his earlier experiments, Aitken produced supersaturation by blowing steam into a large vessel containing the gas to be tested. Later he used an expansion method. Aitken also constructed apparatus for measuring the number of dust particles capable of acting as nuclei of condensation in samples of air.

Since Aitken's experiments, several cloud simulation chambers have been built. Two major approaches are evident. The first approach was characterized by very large chambers in which the designers attempted to extend the time period

of quasiadiabatic expansion of the air by making the surface to volume ratio as small as possible. Special insulating techniques are required for this type of chamber. This method was employed by Findeisen [6] in 1939 and later by R. Gunn [14] in 1952 and was also employed by J. Podzimek [15] in 1964 who operated a modified Findeisen low-pressure chamber. In spite of the improved insulation of the outer wall and of the inner volume, it was not possible to simulate the development of cumulus type clouds more than 1,500 meters above cloud base level and the artificial fog did not persist for more than 15 minutes at a temperature of approximately 0°C . R. Gunn faced similar problems. Currently, Russian scientists are attempting to solve the same kind of problems in several giant cloud chambers built during the past decade [6, 16].

The second method of simulating cloud formation is to control precisely all physical processes in relatively small chambers. Work along these lines began about three decades ago. Only a few scientists have introduced innovations leading to more efficient simulation experiments in small chambers in which the expansion rate, temperature and humidity fields were reliably controlled.

Evans [17] in 1960 was one of the first scientists who tried to eliminate the heat transfer from the wall by cooling the gas and the wall as close to the same rate as possible. This idea was later applied by R. Steele and L. Grant at Colorado State University [18] in 1967 and by

J. Kassner and R. Oetting [19] at UMR (1969) who began the development of such a chamber in 1966. The advantage gained by cooling the wall in synchronization with the cooling of the gas is that the expense of constructing exceedingly large chambers is not necessary. Moreover, the reproducibility and control obtainable in small chambers is much better.

Evans' expansion chamber was in the form of concentric copper spheres. The inner sphere had an 11.5 liter capacity and was cooled by pumping coolant through annular space. Evans used a cooling capacity of 3.5 kW (12,000 Btu/hr) at a suction temperature of -18°C . The maximum cooling rate was $1.5^{\circ}\text{C}/\text{min}$. The temperature of the gas was measured by a copper-constantan thermocouple. It was rather difficult to control the rate of cooling and the total change of temperature of the gas inside the Evans' chamber.

The dynamic cloud chamber developed at Colorado State University was designed to cool the wall at the same rate the gas was cooled by adiabatic expansion. The wall was cooled by means of a refrigeration system. The expansion was programmed by means of a function generator which produced a signal proportional to the desired time temperature curve. The chamber processes were controlled by means of chamber pressure. Expansion rates were adjustable over a range which provided rates of temperature decrease from $0.1^{\circ}\text{C}/\text{min}$ to about $7^{\circ}\text{C}/\text{min}$.

The effort at UMR has been devoted since 1966 to

meticulous design scrutiny and detailed testing of each new design concept. Tebelak [20-21], in 1973 designed and constructed an analog controller for the wall and a gas pressure control. The wall was cooled by thermoelectric modules. He approximated the adiabatic gas law, equation 1.1, by a second order Taylor series expansion and implemented the equation by using a special purpose analog computer. The rate of temperature change was low, less than $0.5^{\circ}\text{C}/\text{min}$. The total change of temperature at that time was only 1.5°C . The controller allowed $2\text{ m}^{\circ}\text{C}$ temperature error between the wall and the gas, or 0.13% of the total temperature change.

In the ideal cloud simulation chamber it should be possible to accurately produce clouds from a saturated atmosphere containing an aerosol fully characterized by a critical activation supersaturation spectrum and the variations of the latter with time. The gas in the chamber must be expanded by an adiabatic process. To accomplish this expansion, the heat transfer between the wall and the gas must be eliminated. The wall temperature and the expansion controller should be able to support a higher rate and a larger change of temperature with reasonable accuracy.

III. DIRECT DIGITAL CONTROL SYSTEM DESIGN

A. DESIGN SPECIFICATION

The main objective of the design is to control the pressure of the gas inside the chamber such that during the cloud simulation experiment it follows a desired profile as closely as possible. The desired pressure profile is generated from the temperature profile using the adiabatic equation 1.1. The pressure profiles are normally negative slope functions with some additional holding modes during the course of the experiment.

Since the pressure transducer is calibrated against a very accurate dead weight, the accuracy of the pressure transducer becomes ± 0.0069 kPa (± 0.001 psi). The expansion control system is designed to meet the following specifications.

1. The settling time must be within 60 seconds.
2. The maximum mean error between the input profile and the output response after 60 seconds must be in the range ± 0.0207 kPa (± 0.003 psi). This error corresponds to ± 17 m⁰C.
3. The maximum rms error between the input profile and the output response, after 60 seconds, must be less than 0.0414 kPa (0.006 psi) corresponding to 34 m⁰C.
4. The maximum rate of change of pressure that can be closely controlled must be at least -0.1242 kPa/s

(-0.018 psi/s) which corresponds to $-6^{\circ}\text{C}/\text{min}$.

5. The controller must be able to handle the total pressure change of 21 kPa (3 psi) or 17°C .

An expansion system which meets the above specifications is adequate for microphysical studies. For a typical expansion the initial temperature and pressure are about room temperature and atmospheric pressure.

B. EXPANSION CONTROL SYSTEM HARDWARE

The expansion control system shown in Figures 1.1 and 1.2 consists of several subsystems. They are briefly described below.

1. The Cloud Simulation Chamber [20]. The cloud simulation chamber is made of aluminum, a ten-sided right prism, 61 centimeters high and 48 centimeters in diameter. It has a volume of 0.11 cubic meter and 1.3 square meter inner wall surface. It is a cooled-type cloud simulation chamber. The maximum rate of change of temperature that can be closely controlled is $-6^{\circ}\text{C}/\text{min}$. The chamber is considered to be a closed vessel but small leaks exist. The leaking time constant is of the order of 400 to 500 seconds. The time constant of the chamber in the expansion mode is about 50 to 60 seconds.

2. The Positive Displacement Uni-Directional Pump. The positive displacement pump is considered as a flow generator. In theory, it is capable of providing constant flow under any pressure. In practice, due to internal leakage, it is characterized by a flow generator and an

internal leakage resistance.

3. The Regulator Tank. The regulator tank, shown in Figure 1.1, is used as a reservoir at the low pressure side of the pump. The tank helps to prevent abrupt changes of pressure across the 3-way valve due to a small change of flow. Its function is similar to that of a capacitor in a power supply.

4. The Storage Tank. The storage tank, shown in Figure 1.1, is used for storing supply gas of the same kind as the sample gas. In compression or in the holding mode of operation, the storage tank will supply gas to the cloud simulation chamber.

5. The 3-Way Infinite Position Rotary Valve. The valve, shown in Figure 1.1, is used to control the flow rate into, or out of, the cloud simulation chamber. The valve aperture is a linear function of the angular displacement [22]. The angular displacement is divided into degrees, 240 degrees in total or -120 to +120 degrees with respect to the center position. Angular position between -120 and 0 degrees are assigned to be the expansion mode. The position at zero degrees is assigned as the closed position. The position between 0 and +120 degrees are assigned to be the compression mode. The valve is driven by the stepping motor. The torque required to rotate the valve is about 0.212 N·m (30 oz-in).

From the results of the performance tests of the valve, the valve has been found to exhibit a small dead zone about

the center position and a saturation zone above ± 30 degrees. The dead zone is small and has no significant effect on the system because the valve operates in the expansion mode most of the time. The gearing inside the valve also causes a small backlash of about 0.2 degree.

6. The Solenoid and Manual Valves. There are three solenoid valves and one manual valve in the expansion system as shown in Figure 1.1. The solenoid valves are numbered 1/03, 1/04 and 1/11. The 1/03 valve is a two way, fixed position, solenoid valve. It is used only when extra air is needed to speed up pressure initialization. It must be reset (closed) during an experiment. The 1/04 valve is a three way fixed position solenoid valve. It is used to route the ventilation of the expanded gas from the chamber to the outside environment. It must be open during a simulation. The 1/11 valve is a two way fixed position solenoid valve. It is used to open or close the chamber under program control. During the cloud simulation it must be open. The manual valve can be used to reduce the flow rate for the operation of the expansion system at very low expansion rates.

7. The Pressure Gauge. The pressure gauge, shown in Figure 1.1, is used for monitoring the pressure inside the storage tank.

8. The Pressure Relief Valve. The pressure relief valve, shown in Figure 1.1, is used to automatically regulate the pressure inside the storage tank.

9. The Stepping Motor and Stepping Motor Interface.

The stepping motor used to drive the rotary valve is a Superior Electric Slo-Syn motor, model M063-FD09. The translator driving system is model STM-1800C. Since the torque required to drive the rotary valve is about 0.212 N·m. (30 oz-in), the start-stop without error curve of the stepping motor provided by the manufacturer indicates that at 0.212 N·m torque the speed must be 1050 steps/s or less. In practice, the friction torque of the valve is not constant. The torque varies non-linearly as a function of the valve position. In addition, the acceleration and deceleration effects [23] cause the stepping motor to skip or overshoot a few steps because of the unbalanced torque. It is found that at the speed of 750 steps/s or less, the stepping error is typically 0 to 4 steps. Consequently, 750 steps/s is chosen to be the base driving frequency of the stepping motor. The stepping motor has 200 steps per revolution, or one step equals 1/200 revolution.

The speed of the stepping motor is adjusted in the stepping motor interface. The purpose of the interface is to accept a digital number output from the NOVA 840 and then convert it into a string of pulses. The number of pulses is equal to the digital output number. One pulse corresponds to one step change of the angular displacement.

The output format of the digital output number must be 12-bit sign-magnitude, shown in Figure 3.1. Bits 0 through 10 give the magnitude of the number to be output. The

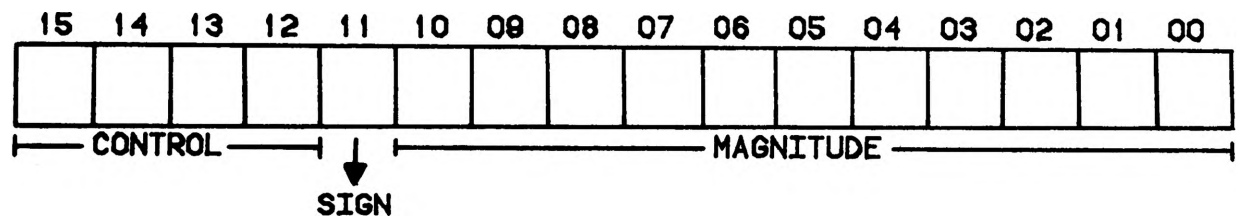


Figure 3.1. The number format of the stepping motor interface.

maximum number can be $2^{11}-1$. The 11th bit is the sign or direction control bit. Bits 12 to 15 are wired OR connected and are used as control bits. A 5 microseconds or longer pulse in any control bit will start the conversion of the stepping motor interface.

The interface is connected to digital output channel #2. Before outputting the desired number of steps to the digital output register, the format must be converted from 16-bit 2's complement binary to 12-bit sign-magnitude binary format. At the same time, a 5 microseconds pulse must be output to the control bits to start the parallel number to serial pulses conversion. The subroutine that handles the format conversion is written in NOVA Assembler called STEPM [24]. The flow chart is shown in Figure 3.2.

The base frequency of the interface determines the speed of the stepping motor. It is set at 750 Hz or 750 steps/s. Currently only 9 bits of magnitude are being implemented. This covers the range of -511 to +511 steps per one output command. It should be noted that the angular displacement of the stepping motor is relative to the previous position; it is not an absolute displacement.

10. The Transducers. The strain gauge pressure transducer is a Statham pressure transducer, model PL80TC-2-350-D, serial #2881. The transducer is a bi-directional differential type, and has a response time of less than 1 ms to step pressure changes. The pressure range is ± 13.8 kPa (± 2 psi) relative to the reference pressure.

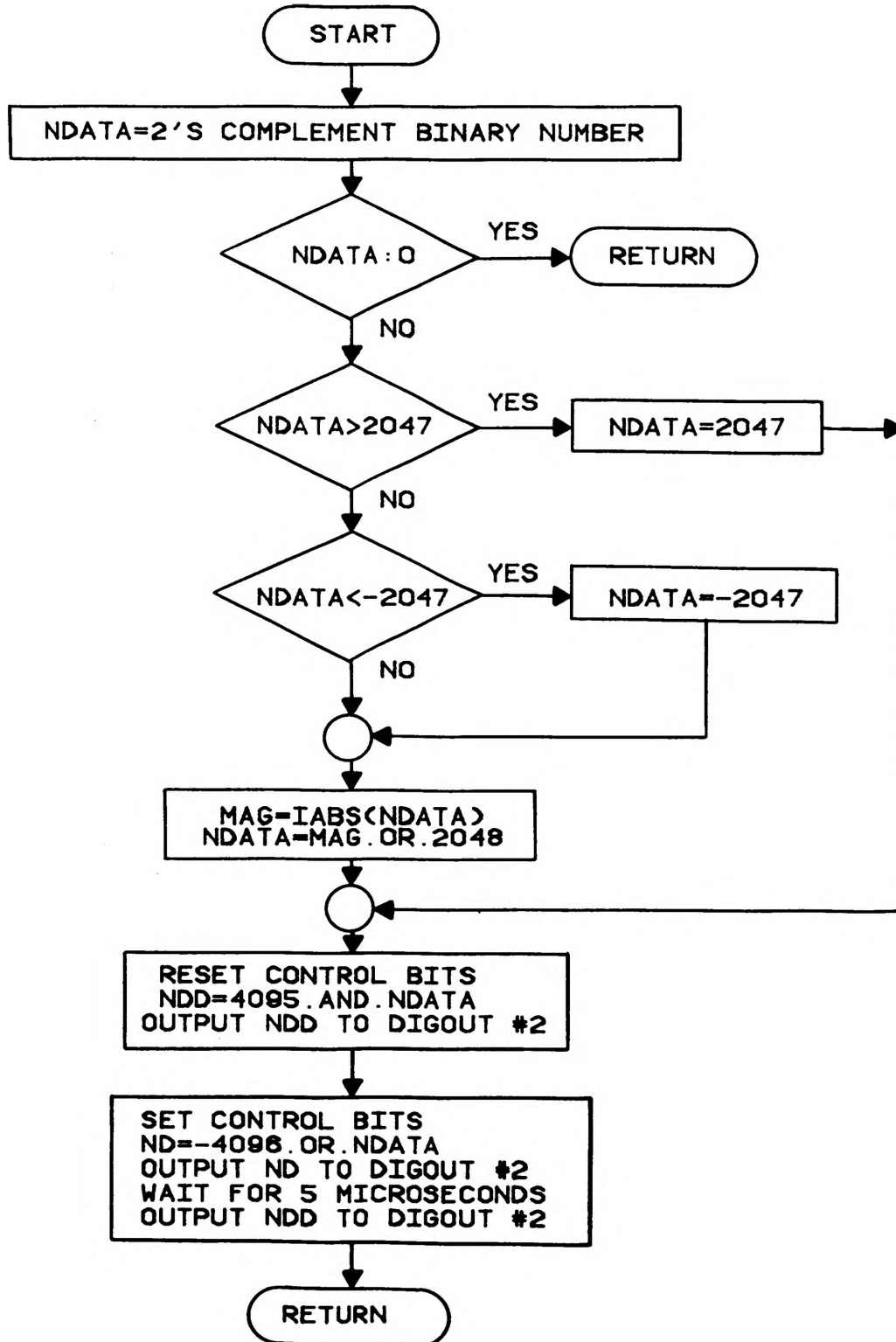


Figure 3.2. The flow chart of the stepping motor interface output routine.

The input resistance is about 350 ohms and the output resistance is about 330 ohms. The resolution is infinitesimal according to the manufacturer. The combined non-linearity and hysteresis are less than $\pm 1\%$ full scale, or ± 0.276 kPa (± 0.04 psi). To obtain better accuracy of the transducer, the transducer is recalibrated against a very accurate dead weight pressure of ± 0.00069 kPa (± 0.0001 psi) accuracy, in the decreasing pressure mode only. Thus the effect of hysteresis can be neglected. The dead weight pressure is a Ruska Instrument dead weight, model 2465-751, serial #18785.

The non-linear characteristic of the pressure transducer is fitted by a second order polynomial using a least square error fit. As a result, the accuracy of the pressure transducer is about ± 0.0069 kPa (± 0.001 psi). The sensitivity is 0.7148 volts/kPa (4.942 volts/psi). The resolution is ultimately limited to 1/2 least significant bit of 15-bit A/D converter or 0.0003125 volts which is equal to 0.000437 kPa (0.0000634 psi). The pressure transducer is connected to channel #9 of the high level A/D converter, Figure 3.3. The transducer is followed by an analog low pass filter which has a cut off frequency at 16 Hz.

The valve position transducer is a potentiometer type position transducer [22]. The valve position is measured by the voltage of a ten-turn potentiometer connected to the shaft of the valve by anti-backlash gearing. The

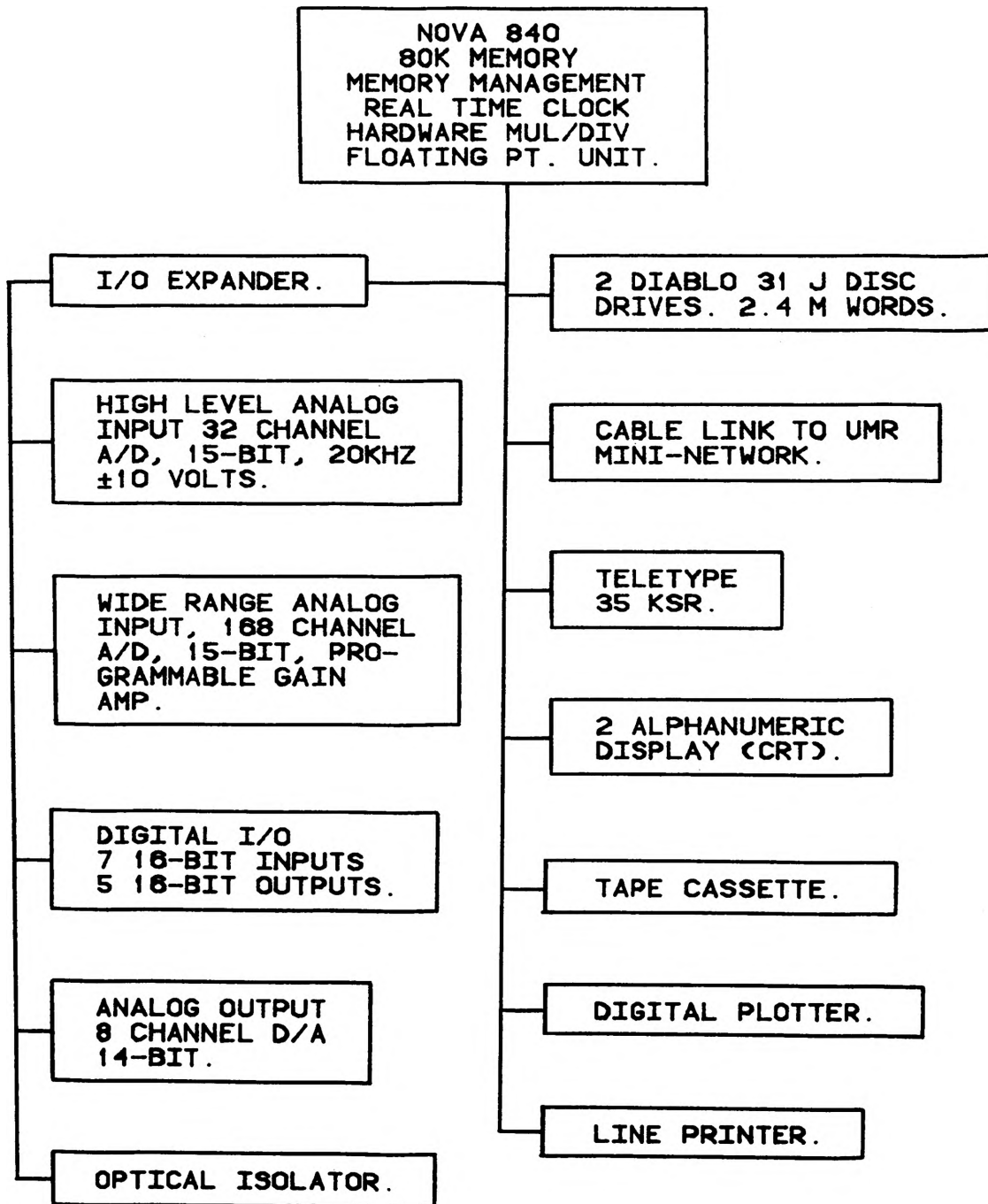


Figure 3.3. The NOVA 840 computer system.

sensitivity is 0.0225 volts/degree. The accuracy is better than ± 0.1 degree. The transducer is connected to the high level A/D converter channel #7 which has an analog low pass filter whose cut off frequency is 8 Hz.

11. The Computer System. The block diagram of the NOVA 840 system at the Cloud Physics Research Center is shown in Figure 3.3. At present, the hardware multiply/divide is being used. Typical execution times of floating point addition, subtraction, multiplication and division are 250, 275, 320 and 340 microseconds, respectively. These times will influence the time needed for identification and control.

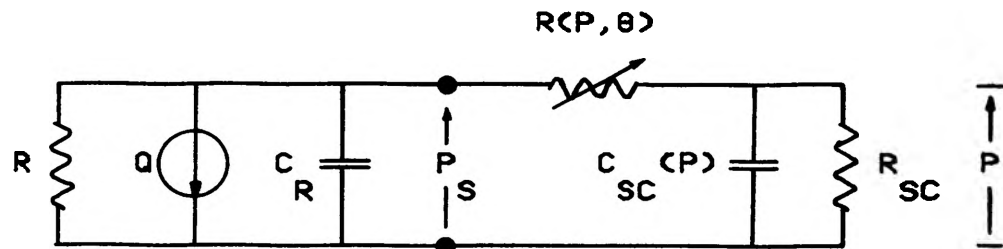
C. MODEL OF THE EXPANSION SYSTEM

A model of the expansion system is required for designing the closed-loop control system. The model can be characterized by the thermodynamic behavior of the system [25]. The analysis indicates that the chamber constitutes a non-linear capacitance as a function of pressure. In addition, the experimental results indicate that the flow rate does not vary linearly as a function of the angular valve position of the rotary valve. Therefore, the expansion system should exhibit multiple non-linearities. These multiple non-linearities are confirmed by the experimental results. Assuming the model of the expansion is finite order, properties like capacitance and resistance of the chamber, the orifice and the valve are lumped. To represent the behavior of the system for the

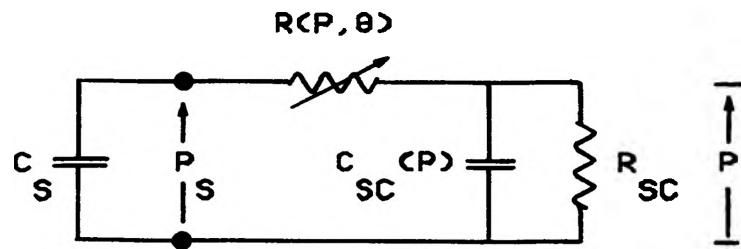
whole range of operation, quasi-linear models are developed, and the values of lumped parameters can be found experimentally [26-28].

The lumped parameter circuit analogy to the expansion system is shown in Figure 3.4. Separate circuits are necessary for each mode of the 3-way infinite position rotary valve. It should be noted that the expansion system is arranged so that the pressure is referenced to room pressure and not the absolute pressure. This arrangement increases the accuracy and simplifies the model of the expansion system since pressures of interest lie fairly near room pressure.

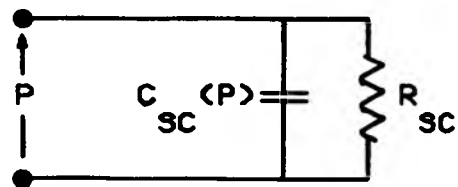
The most important mode of operation is the expansion mode. In Figure 3.4, the R_{SC} represents the lumped leaking resistance of the chamber. The $R(P, \theta)$ represents the variable resistance of the valve as a function of the chamber pressure, P_{SC} , and the angular position of the valve, θ . R_p represents the internal resistance of the pump, and $C_{SC}(P)$ is the cloud simulation chamber lumped capacitance. The regulator tank and the pump produce a pressure source, P_S , across the 3-way infinite position rotary valve. This simplifies the model of the expansion system since it is preferable for a computer-limited application to start with a simplified model. Then the resulting controller synthesized by optimal control theory will require much less computer time than a control law based on a higher order model [29]. The expansion system



(a) EXPANSION MODE



(b) COMPRESSION MODE



(c) CLOSED MODE

Figure 3.4. The electrical analogy of the expansion system.

model is simplified to be a first order system which consists of the pressure source, P_S , the variable resistance valve, $R(P,\theta)$, and the cloud simulation chamber $C_{SC}(P)$. The approximate model, Figure 3.4a, can be written in the form

$$\dot{x}(t) = f(x(t),\theta(t),t) \quad (3.1)$$

$$P(t) = x(t) \quad (3.2)$$

where $x(t)$ is the state variable at time t and $\theta(t)$ is the valve position at time t . This relation can be linearized in the vicinity of an operating point [25]. For a small perturbation about a particular operating point, $\theta_0(t)$ and $x_0(t)$, the linearized equation becomes

$$\delta x(t) = a(t)\delta x(t) + b(t)\delta \theta(t) \quad (3.3)$$

$$\text{where } a(t) = \left. \frac{\partial f(x,\theta,t)}{\partial x} \right|_{\theta=\theta_0(t),x=x_0(t)} \quad \text{and}$$

$$b(t) = \left. \frac{\partial f(x,\theta,t)}{\partial \theta} \right|_{\theta=\theta_0(t),x=x_0(t)} .$$

In classical control systems analysis, either sine waves at various frequencies or step functions are usually used as excitations in order to develop a system model from experimental data. The frequency response or step function response can then be analyzed to obtain the coefficients of differential equations [26].

For the discrete control systems, the dynamic model of a system is assumed to be a difference equation. The

quasi-linear dynamic model equations of the expansion system are

$$x(k+1) = A(k)x(k) + B(k)\theta(k) \quad (3.4)$$

$$P(k) = X(k) \quad (3.5)$$

where $x(k)$ is the discrete state variable, $P(k)$ is the chamber pressure relative to equilibrium pressure (room pressure) at $\theta(k)=0$, $\theta(k)$ is the valve position, $A(k) = A(P(k), \theta(k))$, $B(k) = B(P(k), \theta(k))$ and k is the number of sampling periods. The values of $A(k)$ and $B(k)$ of the difference equation can be obtained experimentally [26]. The sampling period, T , is determined from the sampling theorem (Shannon Theorem) [9]. The sampling period must satisfy the equation

$$T \leq \frac{1}{2} \left(\frac{2\pi}{\omega_e} \right) \quad (3.6)$$

where ω_e is the highest natural frequency of the band limited signal in radians per second. For the expansion system, ω_e is about 1/50 radian per second. Then T must be less than 157 seconds or the sampling frequency must be faster than 0.00637 Hz. In the design, the sampling period has been chosen to be quite small in order to reduce the pressure error caused by the error of the control signal. Theoretically, there is no lower limit on the sampling period but the number and the period of on-line computation tasks limit the minimum sampling period to be only 4

seconds or 0.25 Hz sampling frequency.

From the experimental results, the values of $A(P(k), \theta(k))$ are always less than 0.98 for $P(k)$ between 0 and -27.6 kPa (-4 psi) with respect to room pressure and $\theta(k)$ is between -120 and +120 degrees. This means that the expansion system is always stable in the range of operation [9,30]. The system is also controllable and observable. The first order quasi-linear approximation has a significant advantage in the design of the digital control system in the sense that the complexity of the optimal control analysis has been reduced, which also reduces the required computer time [29].

D. SYSTEM SOFTWARE

1. The Implementation of the Time-Optimal Control. In order to perform an interesting microphysical experiment, the high performance pressure and wall temperature controllers are required by the given specification. In the pressure control case, the pressure error between the desired profile and the pressure response must be minimized. The characteristics of the problem, the system non-linearity and the ramp input function, make it very difficult to have a zero steady state error by using ordinary classical closed-loop control laws. Theoretically, zero steady state error can be obtained from the optimal control law by selecting the right performance index and the right value of weighting parameters. Commonly, the minimum summed-square error (quadratic performance index) and the time-

optimal control yield a zero steady state error for the input ramp function, provided the weighting parameter on the control is zero [11]. The typical performance index of the minimum summed-square error [9,11] is

$$J = \sum_{k=0}^{\infty} [(P(k)-Y(k))^T (P(k)-Y(k))] \quad (3.7)$$

where $P(k)$ and $Y(k)$ are the output response and desired output at sampling instant k , respectively.

For the time-optimal control, given a linear system and an initial state at any point in state space, there exists a control to bring the system from the initial point to the origin in minimum time. If the control is unconstrained, the origin can be reached in one sampling period [9].

The closed-loop control of the expansion system is arranged as shown in Figure 3.5. Here, the linearized transfer function of the expansion system in the expansion mode is the system to be controlled. K and τ , in Figure 3.5 are the linearized gain and time constant of expansion system in the expansion mode, respectively. V_p and θ are pressure voltage and the valve position, respectively.

Since the expansion system is approximated by a first order quasi-linear model, the state feedback gains obtained from the minimum summed-square error control strategy and the time optimal control strategy are exactly the same [9-11]. The time-optimal control is chosen for the design since the analysis of the control is much simpler than the

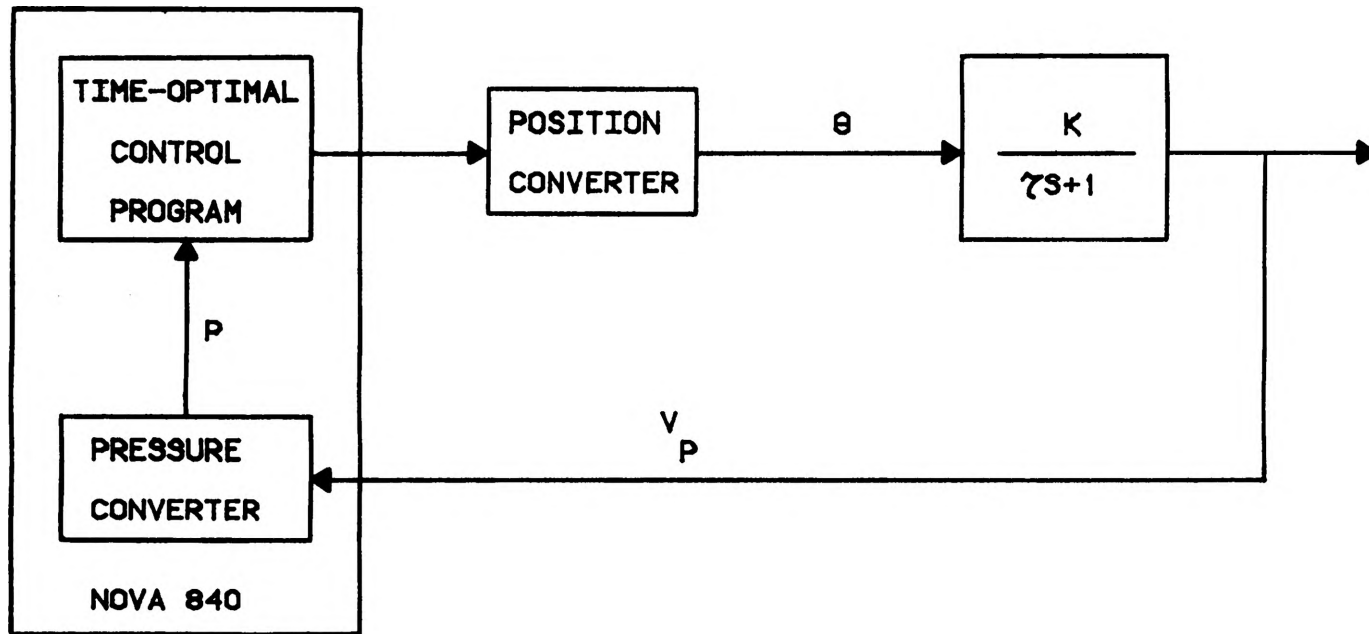


Figure 3.5. Block diagram of the closed-loop digital control of the expansion system.

minimum summed-square error.

In the implementation of the time-optimal control, a particular pressure $P(k)$ is treated as an initial point and the desired final point $P_D(k+1)$ is treated as the origin. The control, $\theta(k)$, that will bring the pressure from the initial point to the origin within minimum time is shown in Figure 3.6, where $GAIN2=1.0/B(P(k),\theta(k))$ and $GAIN1=-GAIN2*A(P(k),\theta(k))$. The values of A and B are needed for the control computation, but they are not constant due to the non-linearities of the system. From the experimental results, the optimal feedback gains are valid only for small perturbations of $P(k)$ and $\theta(k)$. To extend to the full range of operation, a table look-up for the values of A and B as functions of $P(k)$ and $\theta(k)$ was developed. A typical table for the parameters is shown in Table I. At each step of control computation, two dimensional linear interpolations of A and B are obtained from this table for particular values of $P(k)$ and $\theta(k)$. It is found that the error of the pressure response using this table met the design specification only at certain rates of expansion. The validity range of a particular table is small, only ± 0.0104 kPa/s (± 0.0015 psi/s). Therefore, for all expansion rates between 0 and -0.1242 kPa/s, six tables would be needed. Since this requires a large amount of core memory and since searching for table entries requires a large amount of time, this approach has serious drawbacks. Moreover, when any part of the control

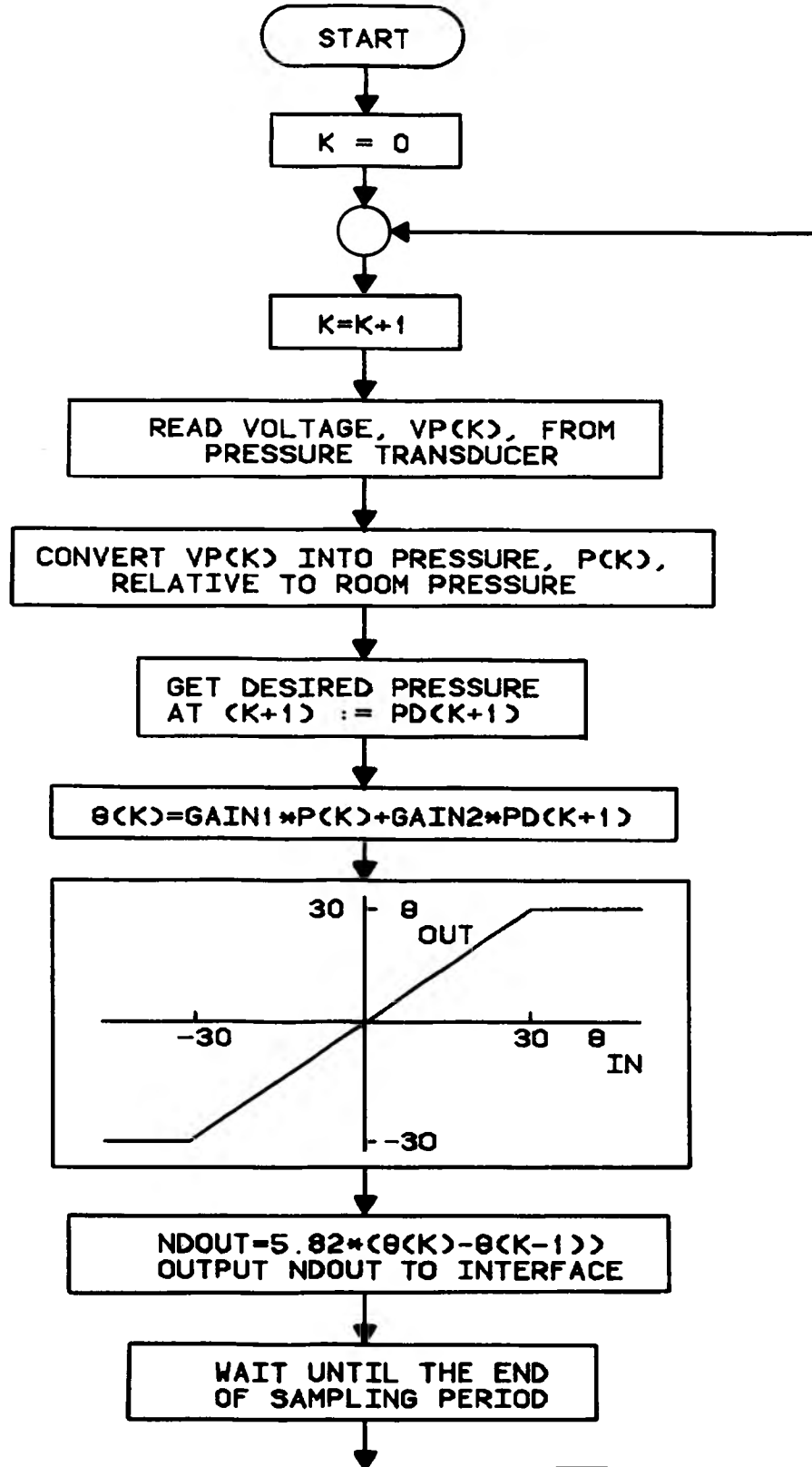


Figure 3.6. The implementation of the time-optimal control algorithm.

TABLE I

TYPICAL TABLE LOOK-UP MODEL OF THE EXPANSION SYSTEM.

 $\Delta\theta = 5$ DEGREES, $\Delta P = 9.66$ kPa (1.4 psi)

P (kPa)	θ (degree)	A	B (kPa/degree)
0	-5	0.958	0.0126
0	-10	0.941	0.0142
0	-15	0.931	0.0137
0	-20	0.920	0.0124
-9.66	-5	0.952	0.0237
-9.66	-10	0.939	0.0207
-9.66	-15	0.929	0.0181
-9.66	-20	0.916	0.0163
-19.32	-5	0.949	0.0270
-19.32	-10	0.943	0.0242
-19.32	-15	0.923	0.0234
-19.32	-20	0.912	0.0207

configuration is changed, all entries in the tables must be reidentified. For example, when the cover of the chamber is opened for service, there is no guarantee that when the cover is replaced and sealed the leakage resistance of the chamber would be the same. Unless the leakage resistance were the same, the characteristics of the chamber would be changed. Consequently, the table look-up approach is not suitable for the development of the cloud simulation pressure control system. The method of table look-up has been dropped and an adaptive control algorithm is implemented. However, the tabulated data gives some useful information in the design of the adaptive control system.

2. The Implementation of the Adaptive Control Algorithm. A real time adaptive control system is not a new subject. In fact, it is used in systems where high quality of control is needed [31]. An adaptive control system has two principal functional elements: a plant to be controlled and a controller where the controller design is based on a nominal but inexact mathematical model of the plant and/or its environment, and a method for altering the controller structure in a dynamic manner. The functional block diagram of the adaptive control system of the expansion system is shown in Figure 1.2. First of all, the on-line (real time) identification of the system parameters is required. There are several published research results [32-36] concerning on-line identification

schemes. The response error of the adaptive control system is directly dependent on the accuracy of the identification scheme. For the time-optimal control of the expansion system, the steady state error will be within ± 0.069 kPa (± 0.01 psi) if the value of A and B of the model converge close to their exact value within one step and, assuming B is correct, A must be accurate within $\pm 1\%$, or assuming A is correct, B must be accurate within $\pm 7\%$.

The linear sequential regression perturbation identification [26] for the quasi-linear model of the expansion system is implemented for the on-line identification scheme, since it minimizes the differences between the model and the actual system responses. It also has closed form equations, so no searching techniques are required. Warner [27] pointed out that this type of identification worked very well for a linear system in the presence of measurement noise, and that the accuracy should increase as the number of data points, N, is increased. It should be noted that for a linear system the parameters converge in one step.

The system of interest in this investigation is non-linear. Consequently, some precaution must be taken when applying the identification method. A non-linear system with a ramp input can be considered as a time-variant linear system. For a first order system, there are two time varying parameters, A and B. The characteristics of the time varying parameters can be divided into

three groups. First is the group of systems in which both A and B are strictly monotone increasing/decreasing in the same direction as a function of time. The second group is the systems which have either constant A and B (linear system), or monotone increasing/decreasing A and B but in opposite directions as a function of time. The third group consists of those systems in which A and B are not monotone, but which can be broken up into time intervals such that within each interval the system falls into either group one or group two. The regression identification can not converge within one step for the systems of the first group. In fact, from the digital simulation the parameters A and B oscillate due to self-compensation of each other. For the second group of systems, the regression identification converges close to the correct values within one step. The expansion system is found to be a system of the third group. It is expected to behave like the mixture of the first two systems.

In the preliminary tests, the regression method has been used for the identification scheme. Figure 3.7 shows the corresponding flow chart of the scheme. From knowledge obtained in applying the table look-up method, the values of A and B are limited to lie between 0.99, 0.89 and 0.027, 0.007 respectively. The adaptive control using this scheme yields a small mean error, less than ± 0.0207 kPa (± 0.003 psi) for rates between $0^{\circ}\text{C}/\text{min}$ and $-6^{\circ}\text{C}/\text{min}$, but the rms error increases from 0.0552 kPa

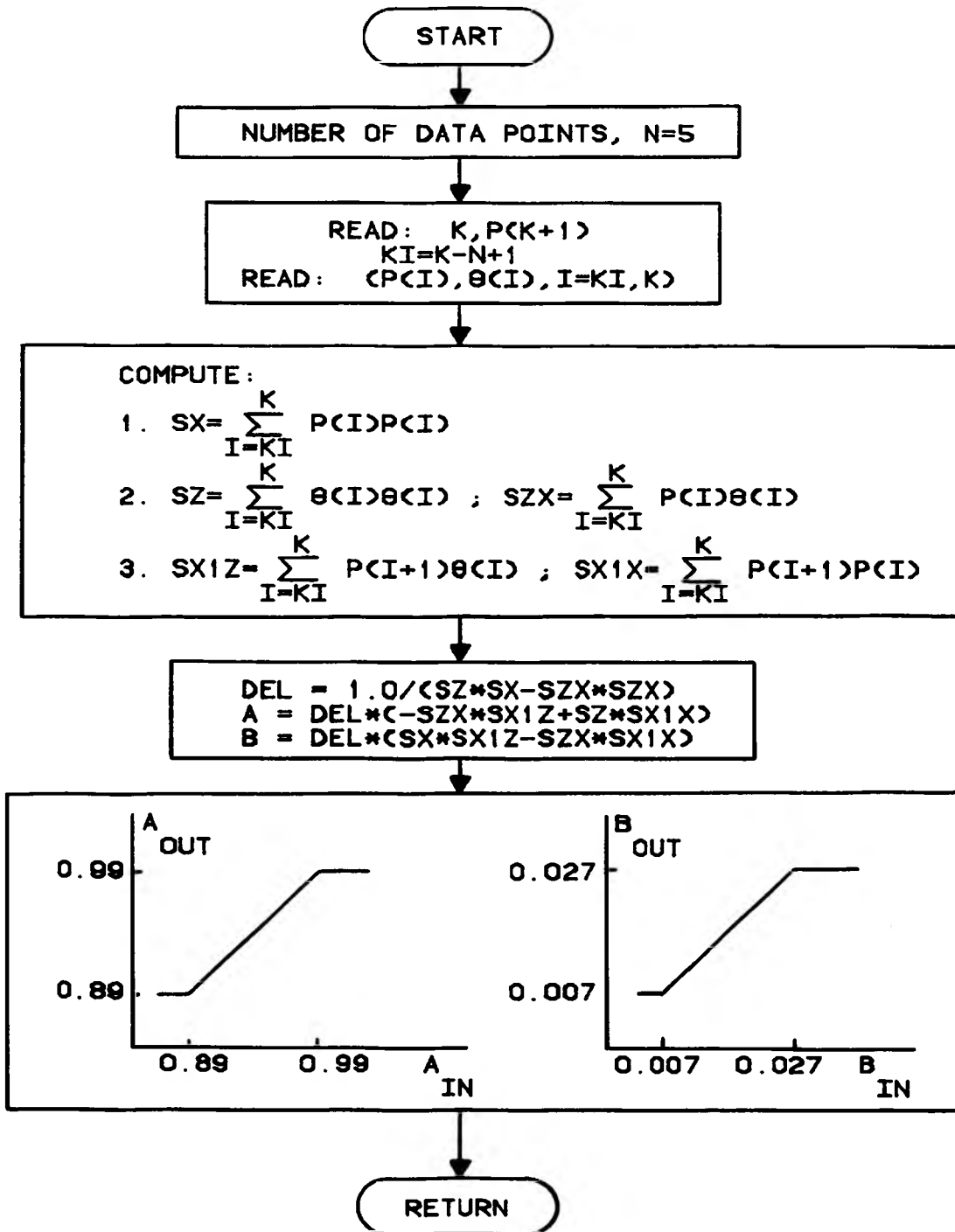


Figure 3.7. The sequential regression identification subroutine.

(0.008 psi) to 0.0828 kPa (0.012 psi) as the rate increases. This scheme can operate without tables over the desired range of operation of the system. The closed-loop pressure response shows some recurrent noise spikes approximately every 40 seconds. The values of $A(P(k), \theta(k))$ and $B(P(k), \theta(k))$ exhibits a wide variation, jumping back and forth. The behavior of $A(P(k), \theta(k))$ and $B(P(k), \theta(k))$ are shown in Figure 3.8 and 3.9, respectively. Five data points are used in the sequential regression identification scheme. It is evident that the larger the number of data points, N , the smoother the regression. But if N is too large, the past data will dominate the present data. This introduces a certain offset of the parameters and leads to increasing the offset of the pressure response. Again, from the table look-up results, it is known that the model parameters change slowly with time. It can be assumed that the real values of parameters also change slowly with time. Assuming the oscillation of A and B are due to the presence of high frequency noise introduced by an imperfect identification scheme, the high frequency oscillation can be filtered out by first order low pass digital filters. The parameters become

$$A(P(k), \theta(k)) = A(k) = AFILTER * A(k-1) + BFILTER * A_{IDENT} \quad (3.8)$$

$$B(P(k), \theta(k)) = B(k) = AFILTER * B(k-1) + BFILTER * B_{IDENT} \quad (3.9)$$

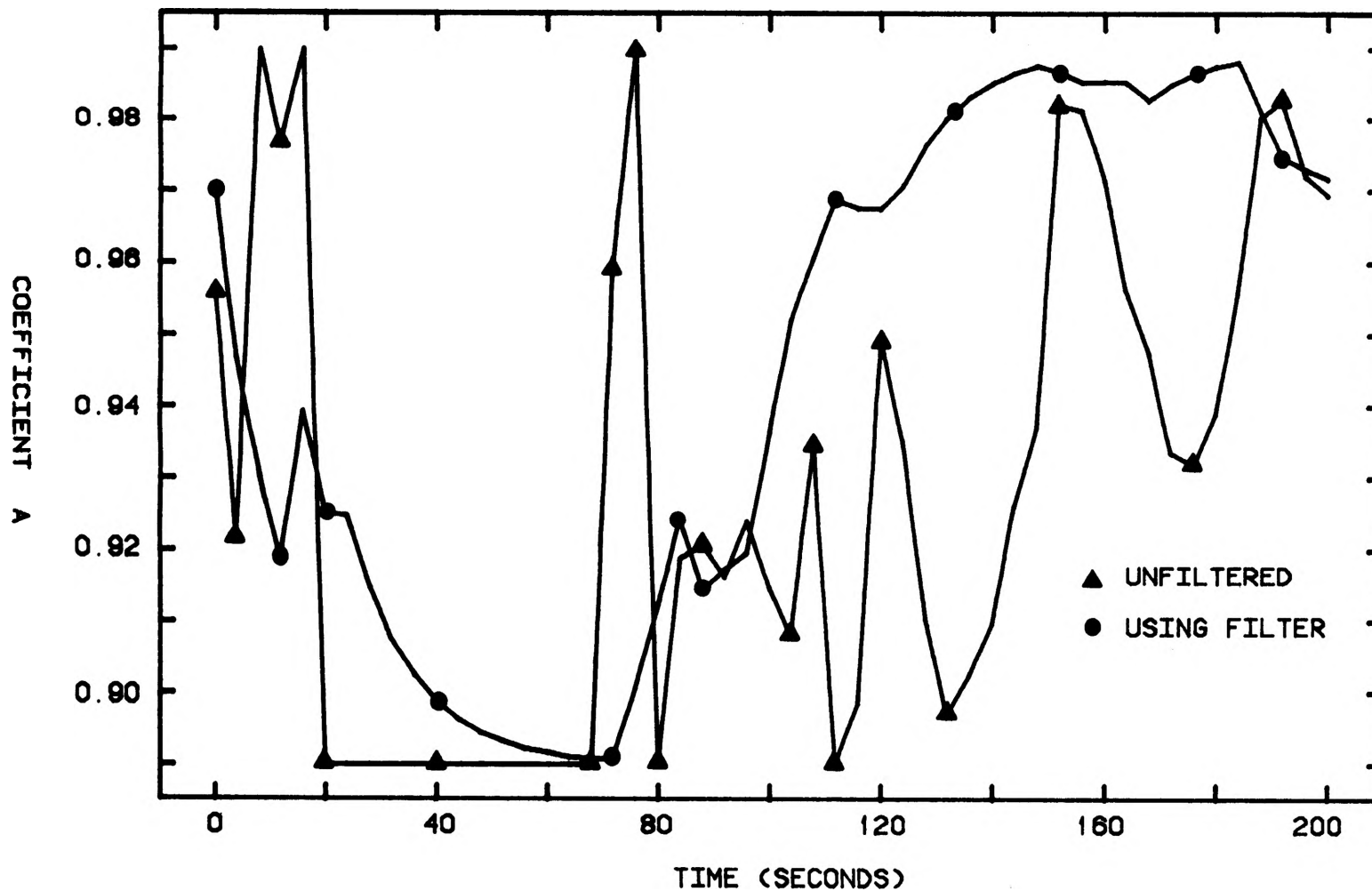


Figure 3.8. The behavior of the coefficient A as a function of time. The rate of expansion is $-4^{\circ}\text{C}/\text{min}$.

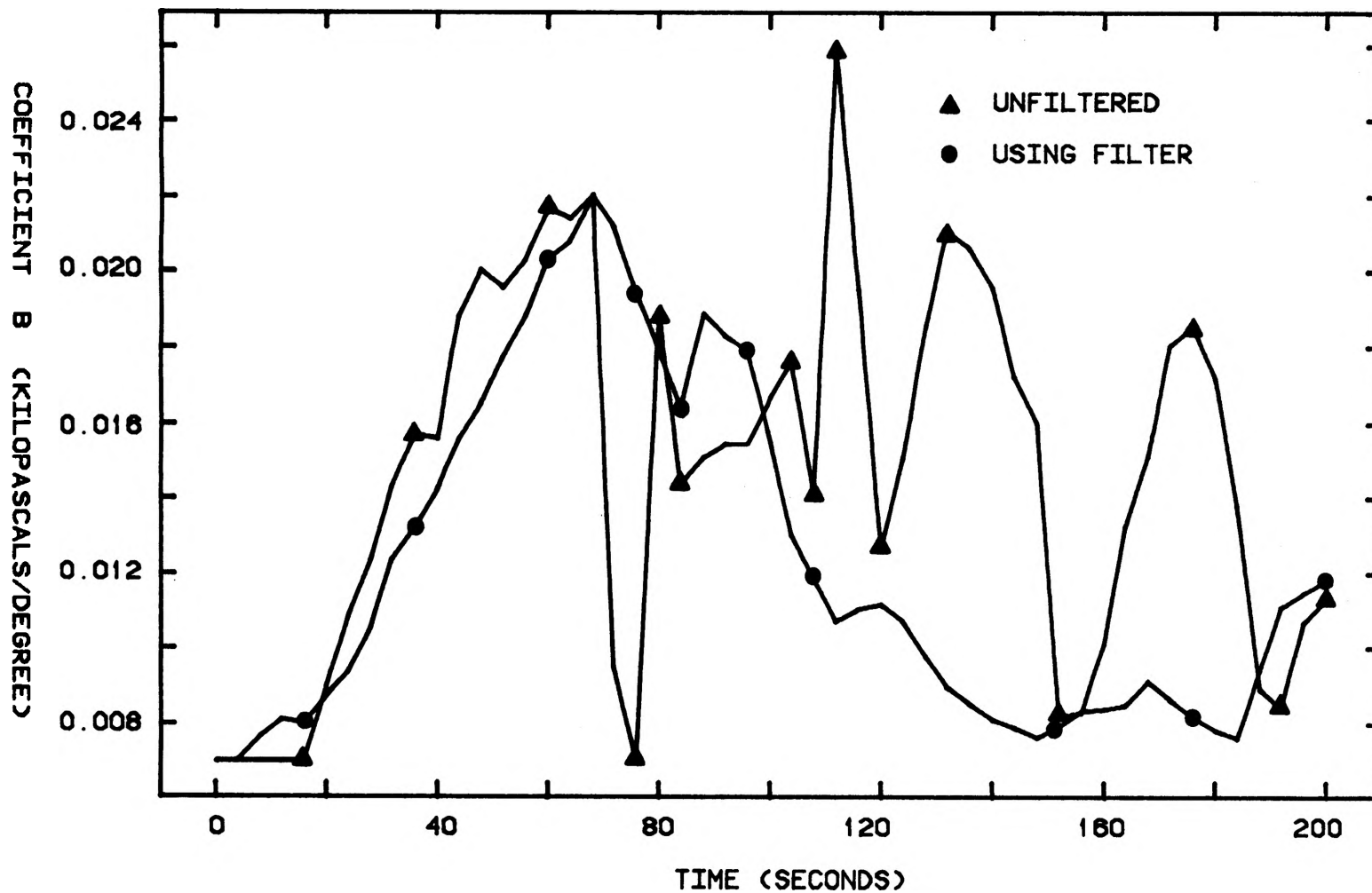


Figure 3.9. The behavior of the coefficient B as a function of time. The rate of expansion is $-4^{\circ}\text{C}/\text{min}$.

where $BFILTER=1.0-AFILTER$ and $AFILTER$ must vary with the rate of change of pressure in kPa/s or temperature in $^{\circ}C/min$. The block diagram of the identification scheme with low pass filter is shown in Figure 3.10. The reason that the value of $AFILTER$ varies with the rate of change of pressure or temperature is that the change of $A(k)$ and $B(k)$ can be approximated by ramp functions. The low pass filter usually introduces offsets at steady state when the input is a ramp. The offset may be kept small or held constant by varying the cut off frequency of the filter. The values of $AFILTER$ are found experimentally and are shown in the Table II. The comparison between the unfiltered and the filtered curves of A and B are shown in Figure 3.8 and 3.9, respectively.

After the low pass filters are employed, the results indicate that the closed-loop control system has improved. The rms error is reduced to below 0.0414 kPa (0.006 psi) for rates from $0^{\circ}C/min$ to $-6^{\circ}C/min$.

3. System Programming. The control program and other programs required to run the cloud simulation chamber are written using multitasking concepts [37]. The programs are written in separate small programs called tasks. A task is defined as a logically complete execution path through a user program that demands use of system resources such as peripheral devices for I/O or simply CPU control work; task execution may occur independently and asynchronously with other tasks. In the multitask

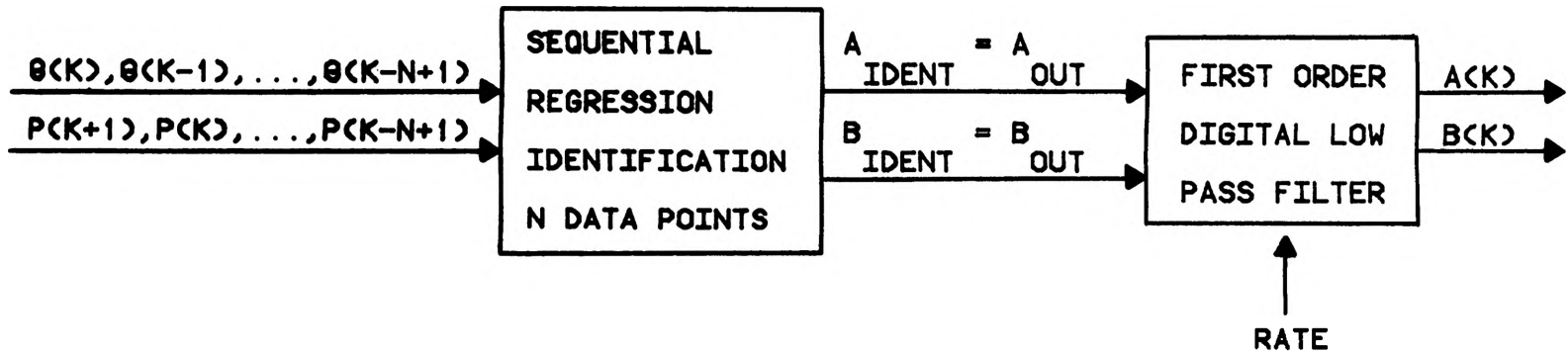


Figure 3.10. The block diagram of overall identification scheme.

TABLE II
EXPERIMENTAL VALUES OF AFILTER AND BFILTER

RATE (°C/min)	AFILTER	BFILTER
0 to -2	0.86	0.14
-2 to -4	0.71	0.29
-4 to -6	0.56	0.44

environment, each task competes simultaneously for the use of system resources. At any single moment, only one task receives CPU control and the desired resources. The allocation of tasks depends on their priority and the readiness to use the resources. A task scheduler governs the transfer of control to each task. All tasks are synchronized to the RTC (real time clock). For more detail, see Chapter 4, Part II, of reference [37].

When a task is activated, by FTASK or ITASK statements, it enters the ready state and competes with other ready tasks for control of the processor based on assigned priorities. The wall temperature output task, called TWALL [24], has the highest priority among other tasks since it is the most important task and the execution time is very short. The pressure control task, called PRESC [24], has the second highest priority. The priority for the rest of the tasks are assigned according to their functional importance.

The main cloud simulation program called SCPROG3 [24] consists of statements activating all the tasks. For the pressure control task a subroutine PREPAR [24] is called to initialize the variables, read in parameters and open a data file to store the experimental results. The flowchart of PREPAR is shown in Figure 3.11. Next the task PRESC, the expansion control task, is activated by the main program. The flowchart of PRESC is shown in Figure 3.12. The sampling period (cycle event) of task PRESC is 4

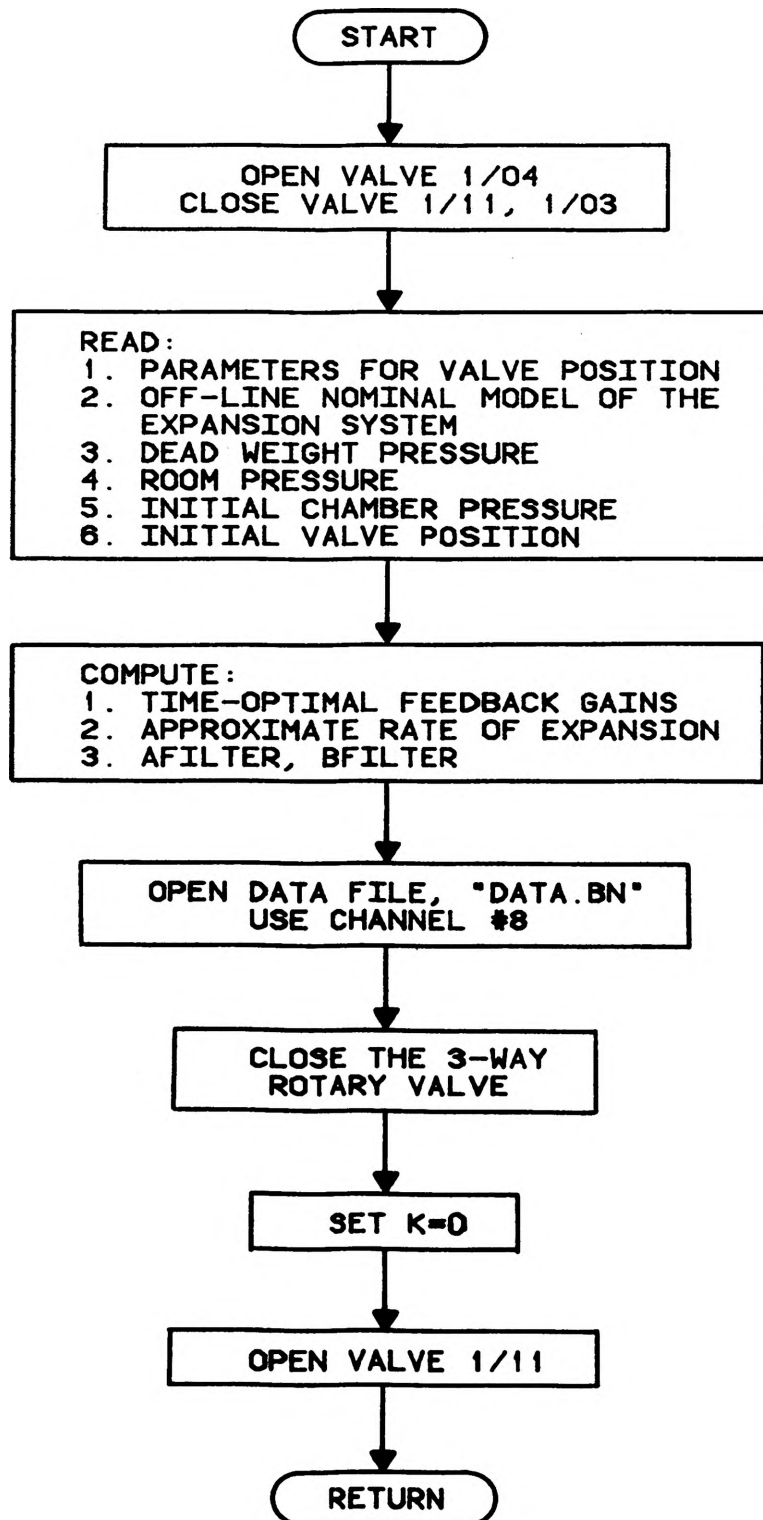


Figure 3.11. The flow chart of the subroutine PREPAR

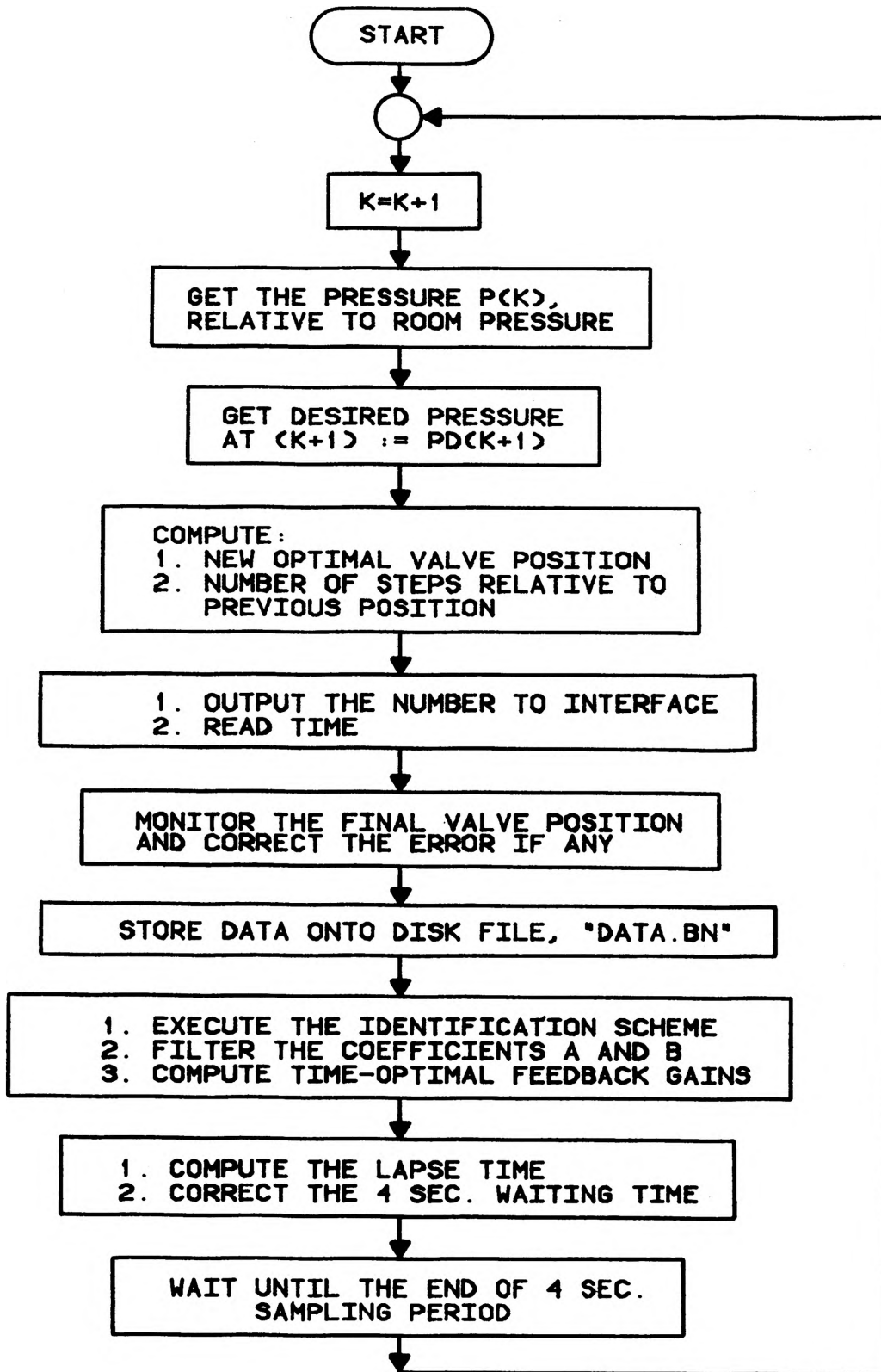


Figure 3.12. The flow chart of PRESC

seconds. The execution time of the time-optimal control computation is about 20 ms. The new valve position is updated via the stepping motor interface. Then the computer waits until the completion of the stepping motor movement and corrects the valve position error if there is any. It takes about 250 ms for this execution. The identification and filtering take place after the completion of the correction of the valve position and require less than 50 ms computation time. The total time occupied by PRESC is about 320 ms, which is about 8% of total available time. The rest of the available time can be used for the execution of other tasks, primarily taking and storing data relating to the aspects of the experiment. The control tasks are given highest priority for the simple reason that other data is useless unless good control of the experiment is achieved.

IV. EXPERIMENTAL RESULTS

Performance tests of the expansion control system are accomplished by a dry adiabatic expansion in which the wall and the gas are cooled at the same rate by using the adiabatic equation, equation 1.1. The program SCPROG [24] is used to prepare the chamber; the program SCPROG2 [24] proceeds after the completion of SCPROG. SCPROG2 holds the pressure and the wall temperature at their equilibrium states before proceeding to SCPROG3 [24], which computes the control and performs other tasks. The input to the wall temperature controller is output via the D/A converter channel #7. At the same time the computer monitors and controls the chamber pressure. The desired and output pressure responses are recorded onto a disk file named "DATA.BN".

To test the convergence of the sequential regression identification scheme, the initial values of A and B are set to be 0.5 and 0.03, respectively. These values are about 50% and 100% off the nominal values. The rate of expansion is set at -0.0828 kPa/s (-0.012 psi/s) or -4°C/min. Figures 4.1, 4.2 and 4.3 show the results of the coefficients A and B and the pressure error, respectively. Evidently, from the error curve, the identification scheme converges within 60 seconds. It should be noted that the response between two discrete data points is approximated by a straight line connecting

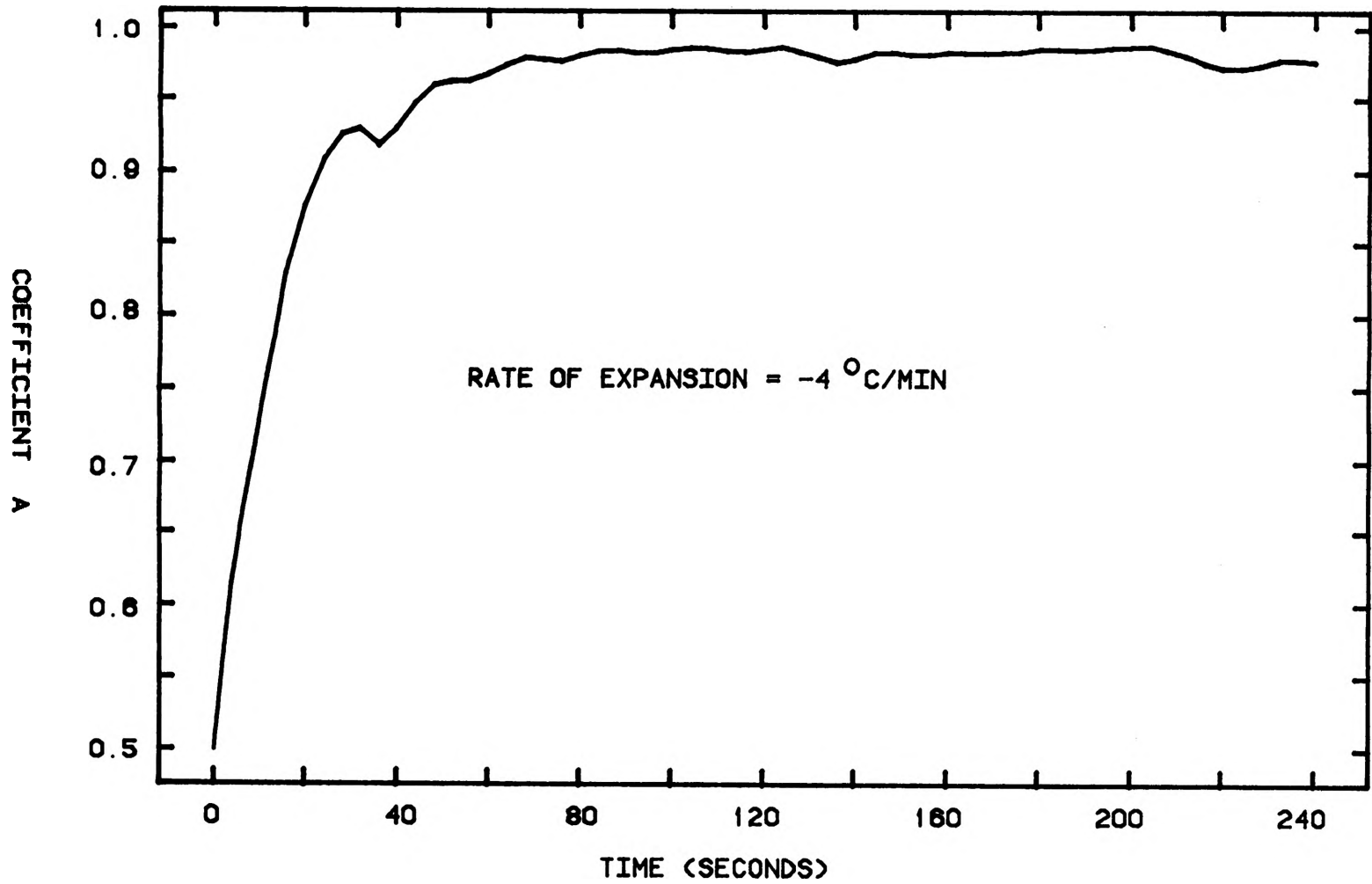


Figure 4.1. The coefficient A when A and B are initially set at 0.5 and 0.03, respectively.

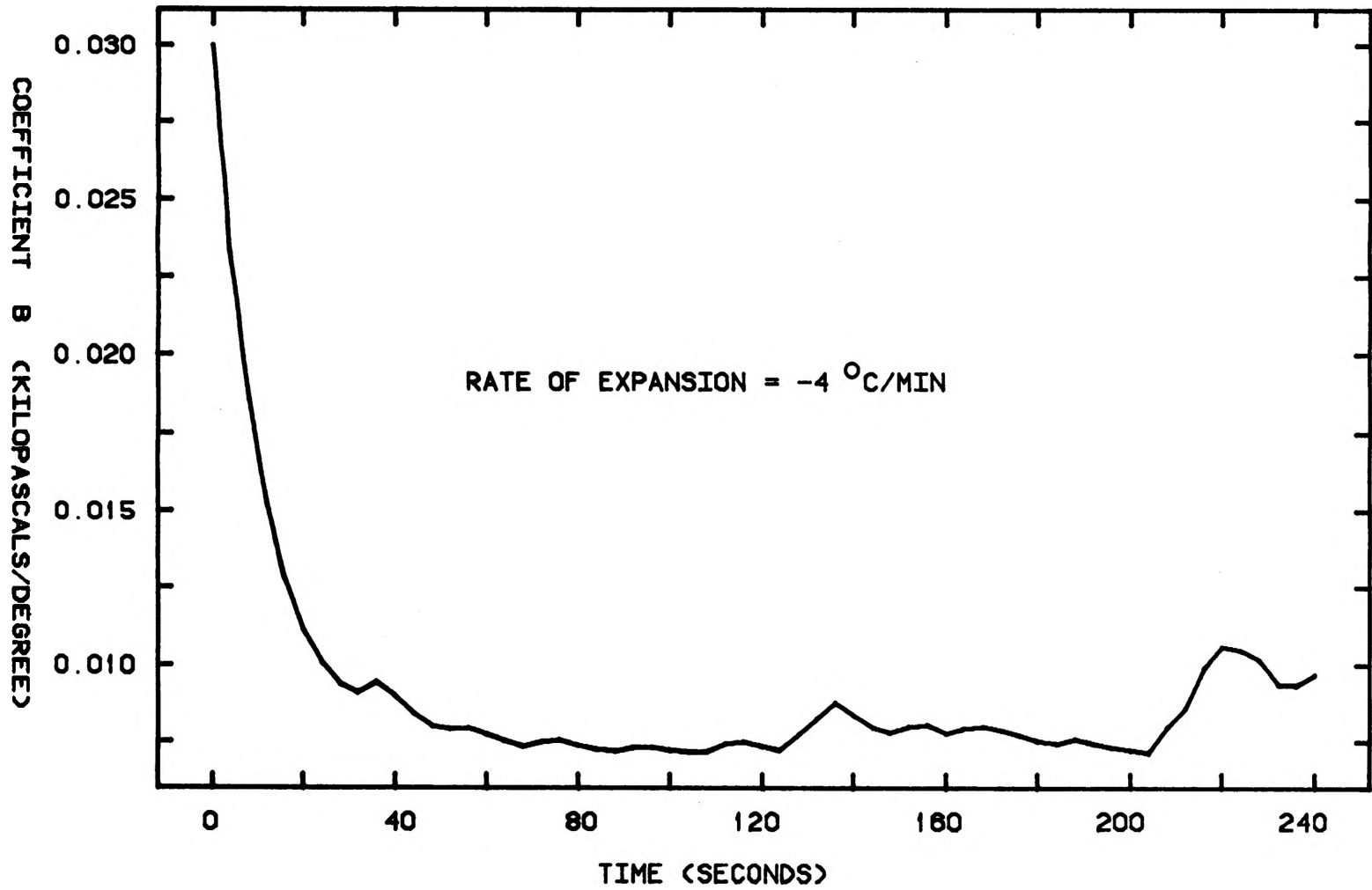


Figure 4.2. The coefficient B when A and B are initially set at 0.5 and 0.03, respectively.

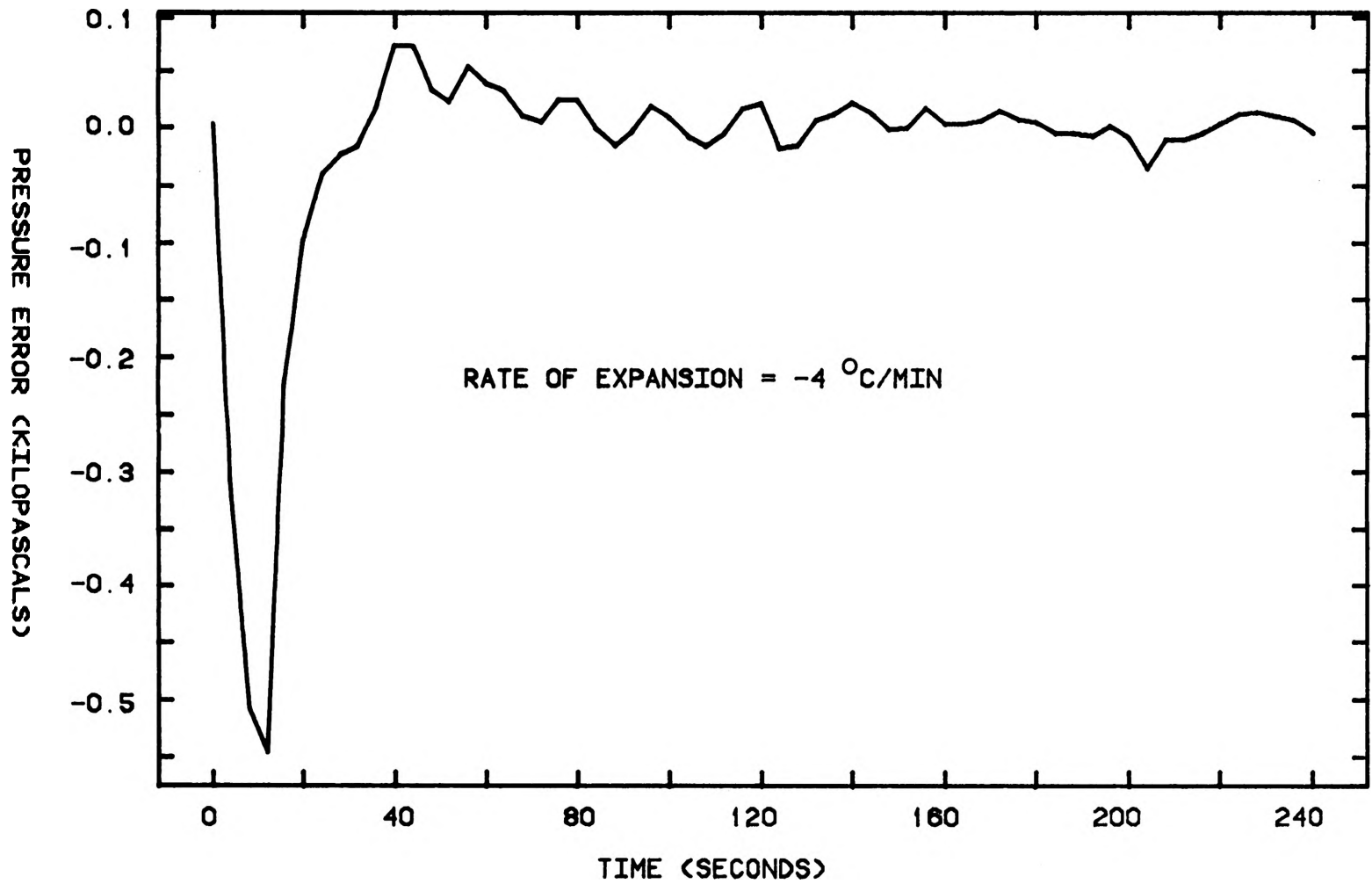


Figure 4.3. The error of the pressure response when A and B are initially set at 0.5 and 0.03, respectively.

the two points. To guarantee that the response between the sampling period has no oscillation, the pressure is recorded every 2 seconds instead of 4 seconds. The pressure response and the pressure error, in Figure 4.4 and 4.5, indicate that there is no significant oscillation between the sampling instant. The straight line approximation between two consecutive data points is acceptable.

Figures 4.6 to 4.9 show the pressure response, the pressure error and the coefficients A and B of the expansion control system at the rate of expansion of -0.1242 kPa/s (-0.018 psi/s) or $-6^{\circ}\text{C}/\text{min}$. Figure 4.10 to 4.13 and 4.14 to 4.17 show the same set of curves but at the rate of -0.0828 kPa/s (-0.012 psi/s) or $-4^{\circ}\text{C}/\text{min}$ and -0.0414 kPa/s (-0.006 psi/s) or $-2^{\circ}\text{C}/\text{min}$, respectively. The results indicate that the mean and rms error of the pressure responses at steady state or after 60 seconds are well below ± 0.0207 kPa (± 0.003 psi) and 0.0414 kPa (0.006 psi), respectively. The total change of pressure is 20.7 kPa (3 psi) except at -0.1242 kPa/s where the total change of pressure that can be closely controlled is about 18.6 kPa (2.7 psi). This is due to the limited pumping capacity of the pump.

Figures 4.18 and 4.19 show the pressure response and the pressure error when the holding mode is incorporated into the desired pressure profile. The initial holding time is 60 seconds. The expansion proceeds at the rate of -0.0828 kPa/s (-0.012 psi/s) for 100 seconds. The final

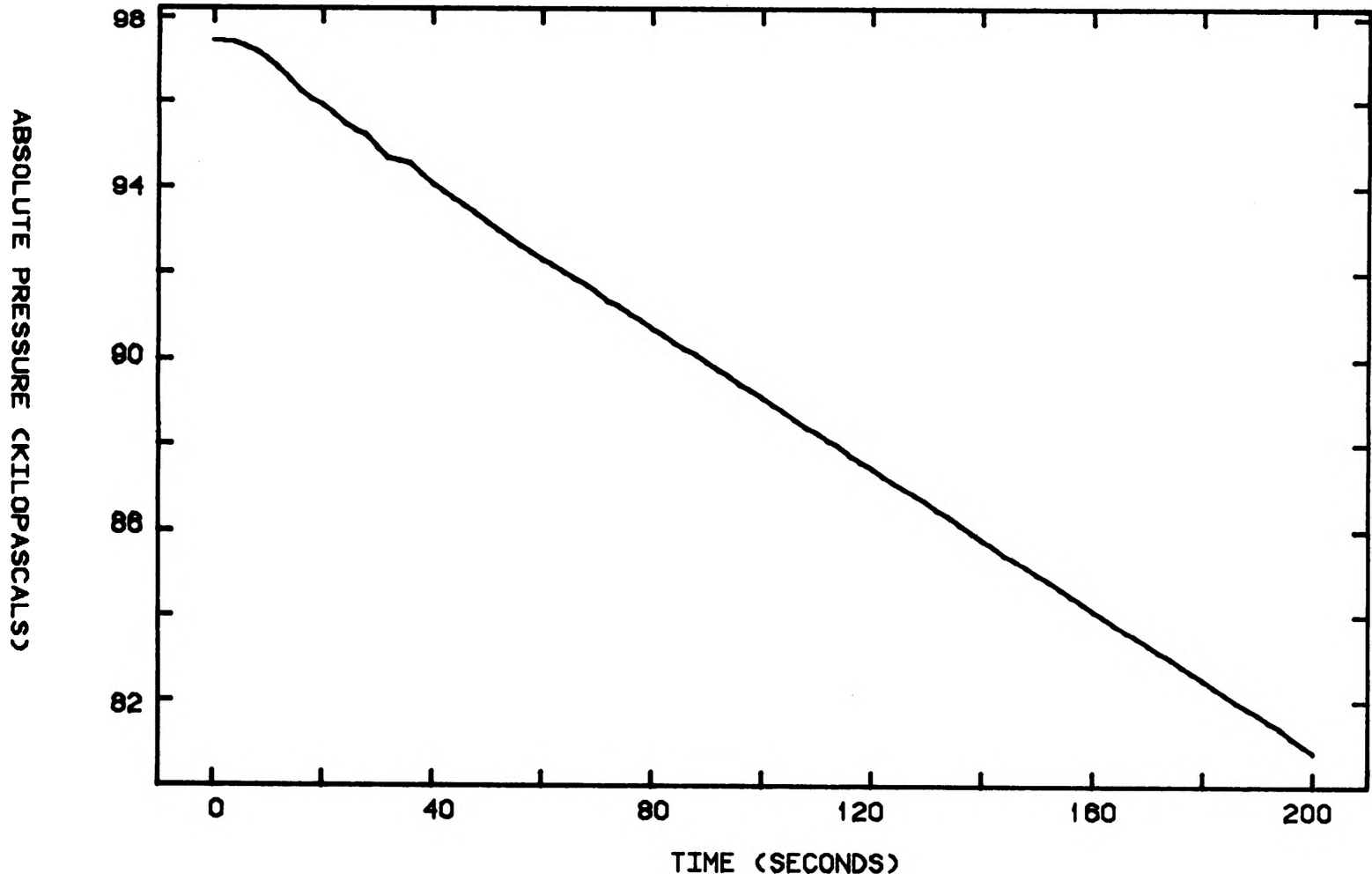


Figure 4.4. The pressure response when being recorded every 2 seconds.

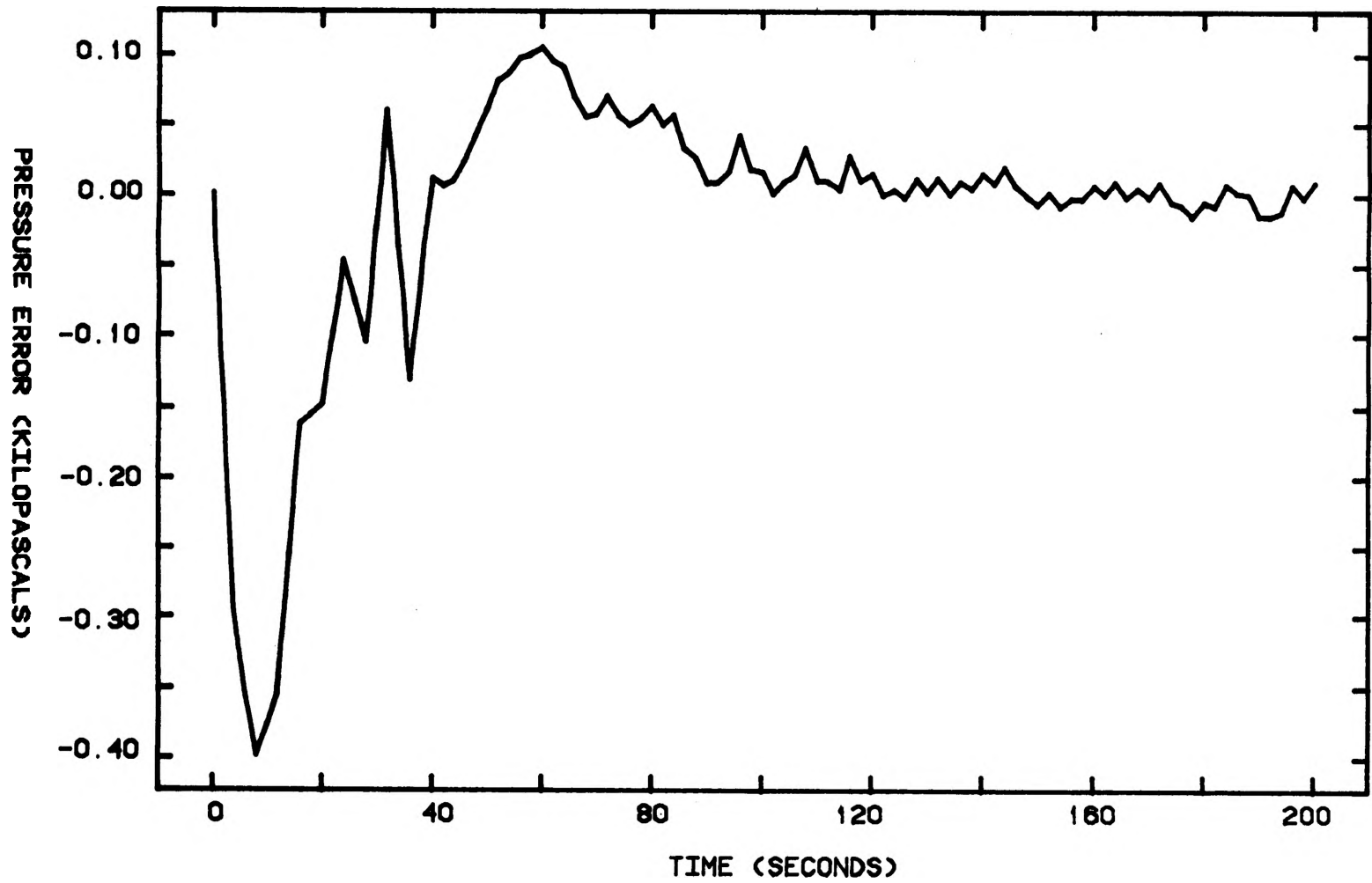


Figure 4.5. The pressure error when being recorded every 2 seconds.

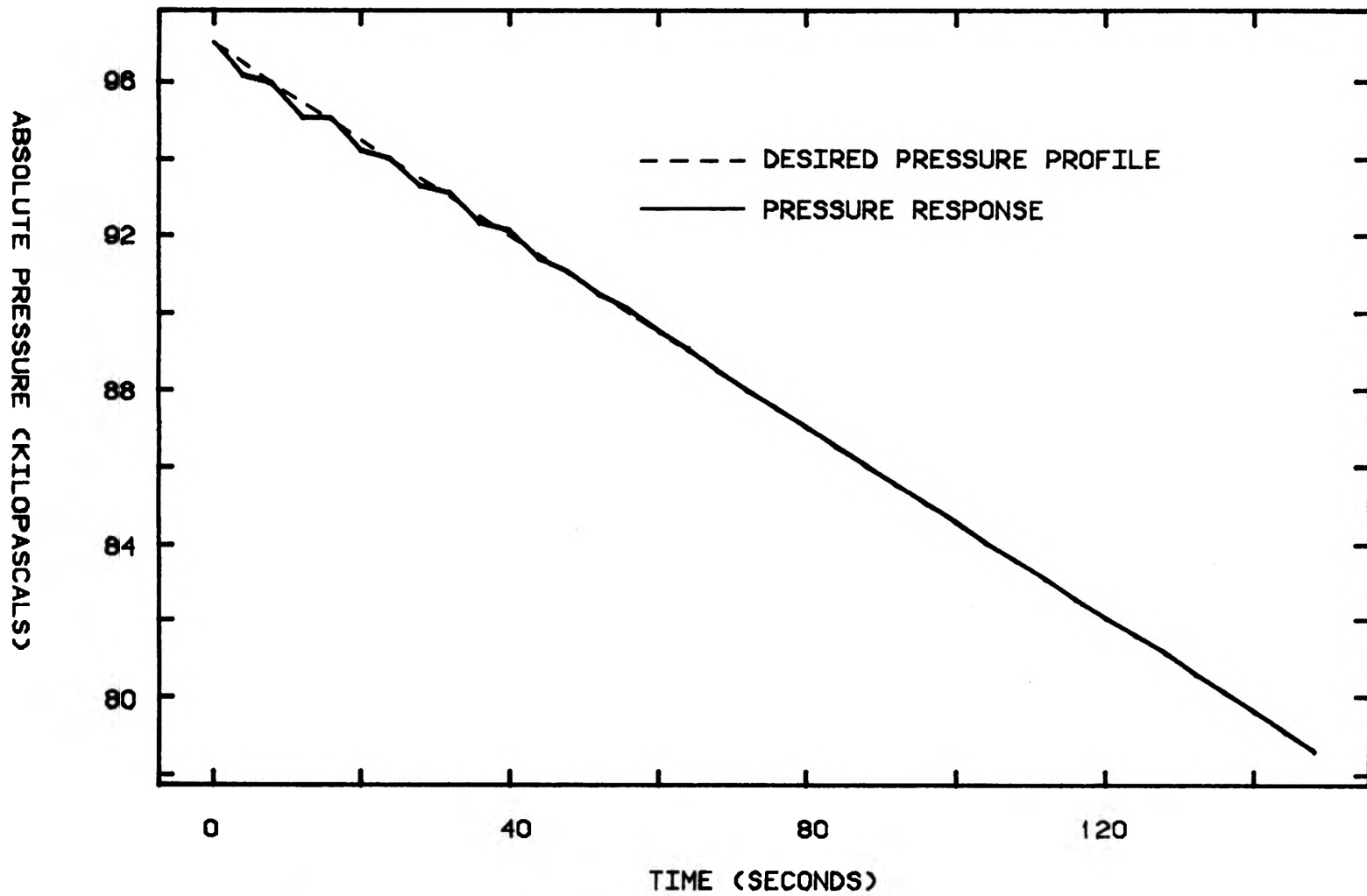


Figure 4.6. The pressure response at the rate of expansion of -0.1242 kPa/s or $-6^{\circ}\text{C}/\text{min}$.

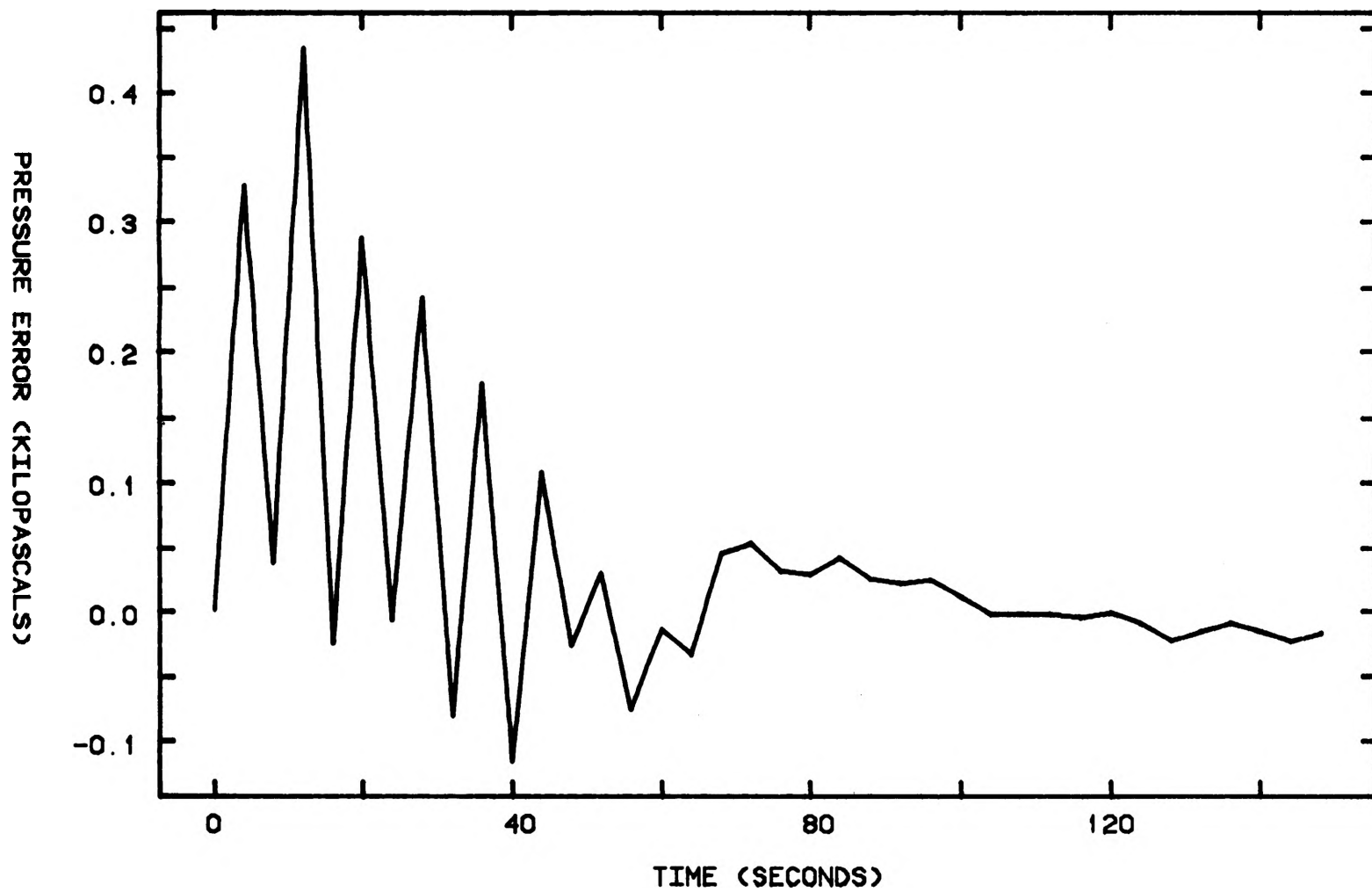


Figure 4.7. The pressure error at the rate of expansion of -0.1242 kPa/s or -6°C/min .

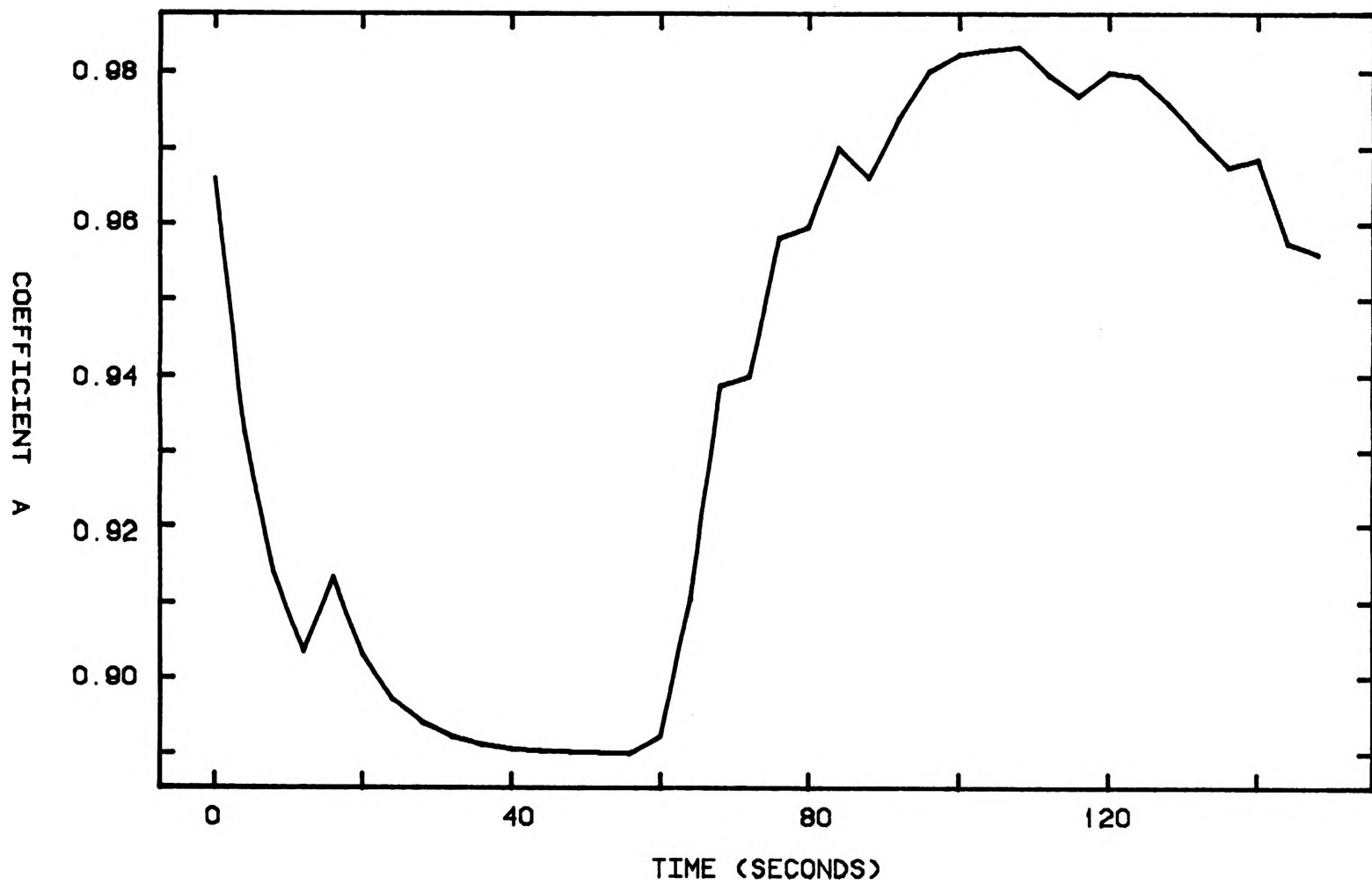


Figure 4.8. The coefficient A at the expansion rate of -0.1242 kPa/s or $-6^{\circ}\text{C}/\text{min}$.

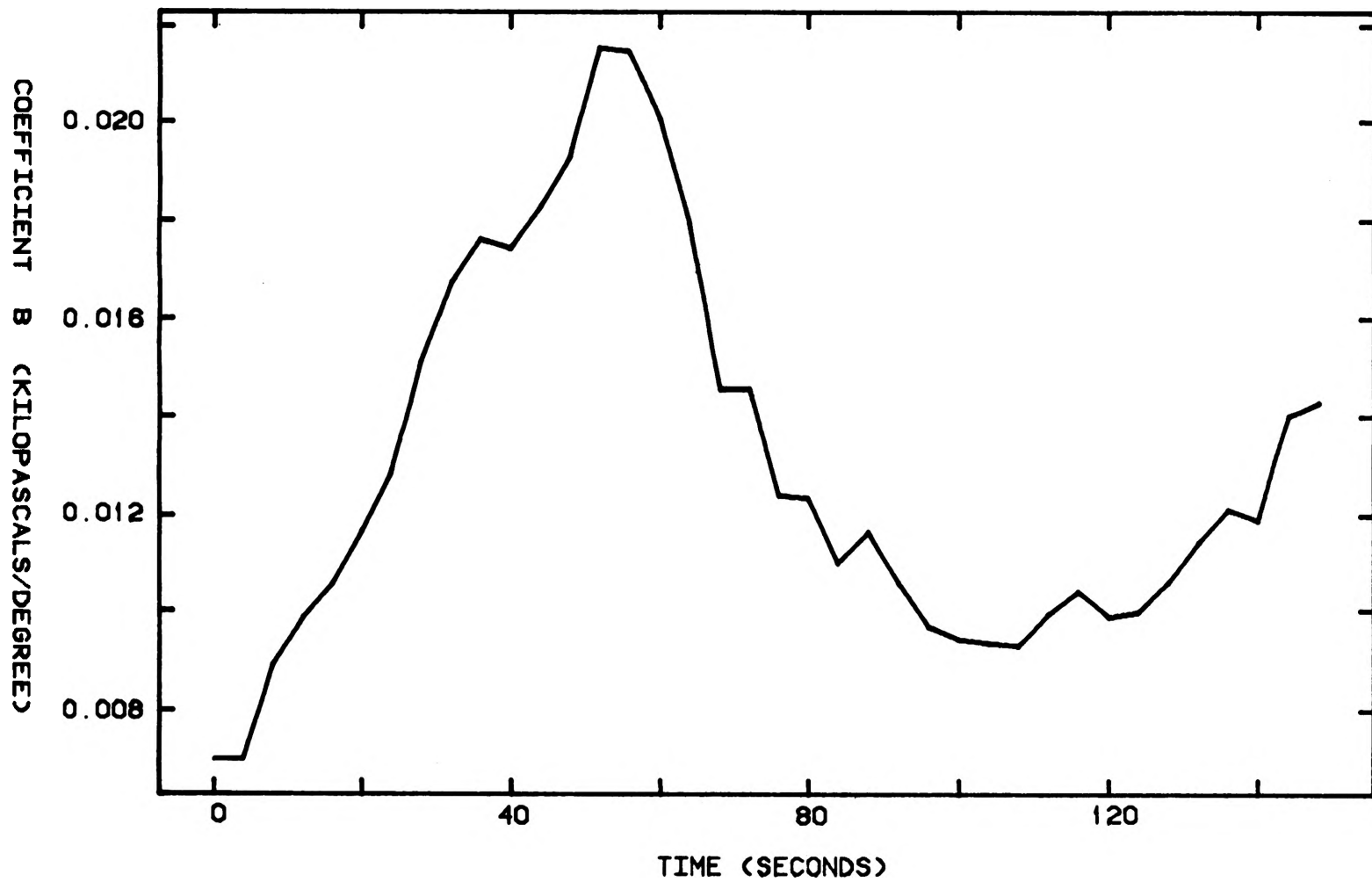


Figure 4.9. The coefficient B at the expansion rate of -0.1242 kPa/s or -6°C/min .

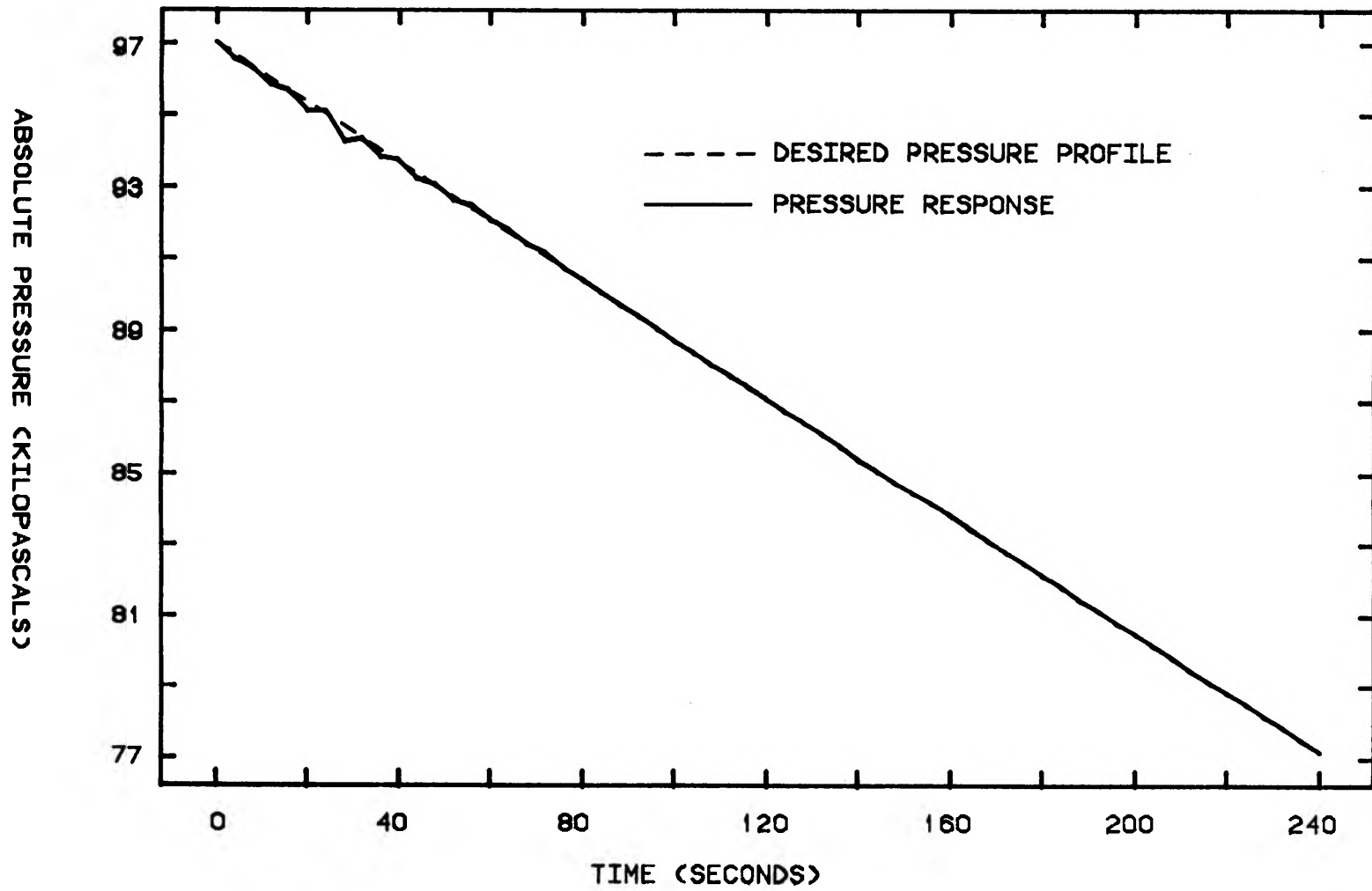


Figure 4.10. The pressure response at the expansion rate of -0.0828 kPa/s or $-4^{\circ}\text{C}/\text{min}$.

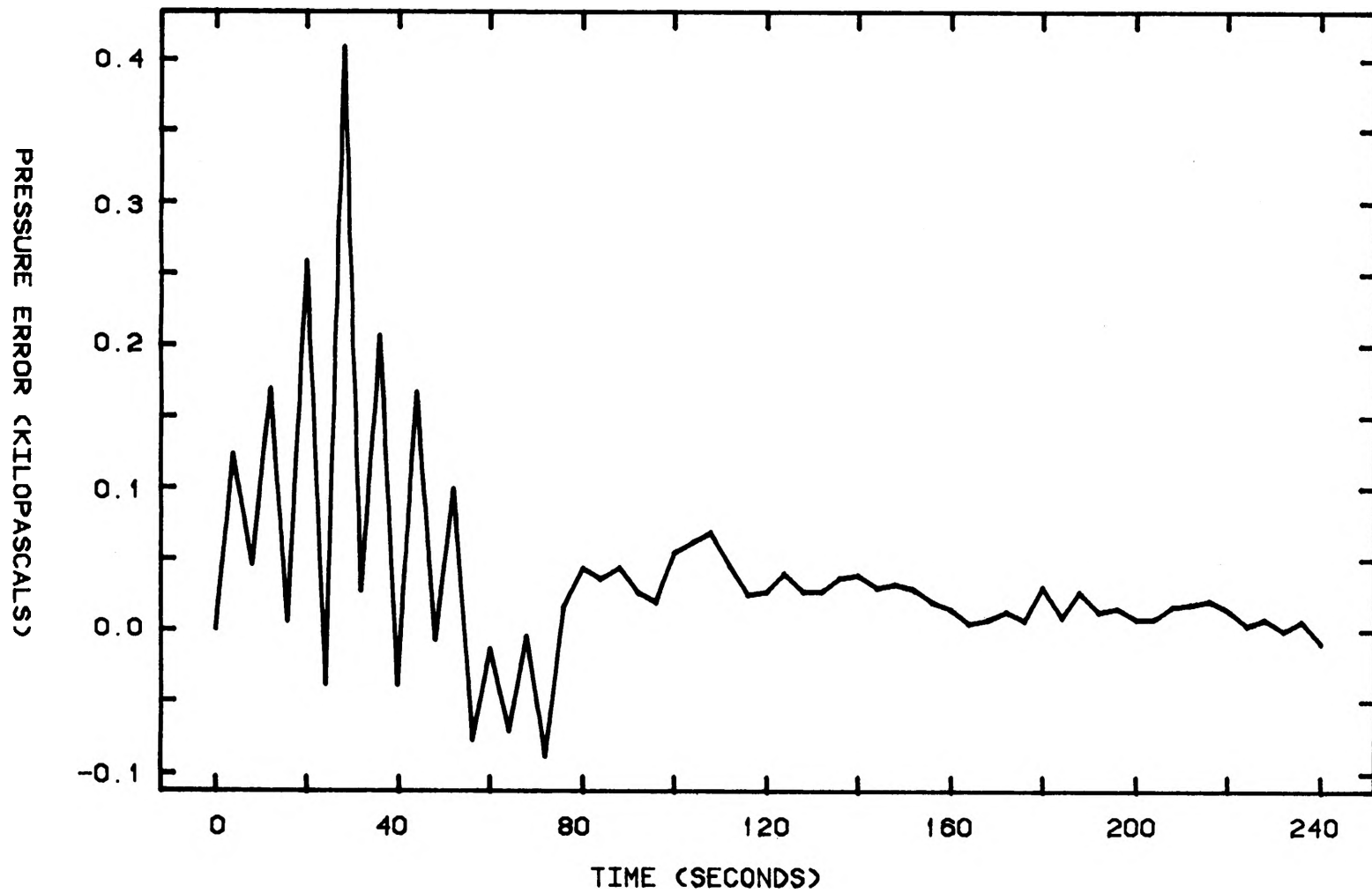


Figure 4.11. The pressure error at the expansion rate of -0.0828 kPa/s or $-4^{\circ}\text{C}/\text{min}$.

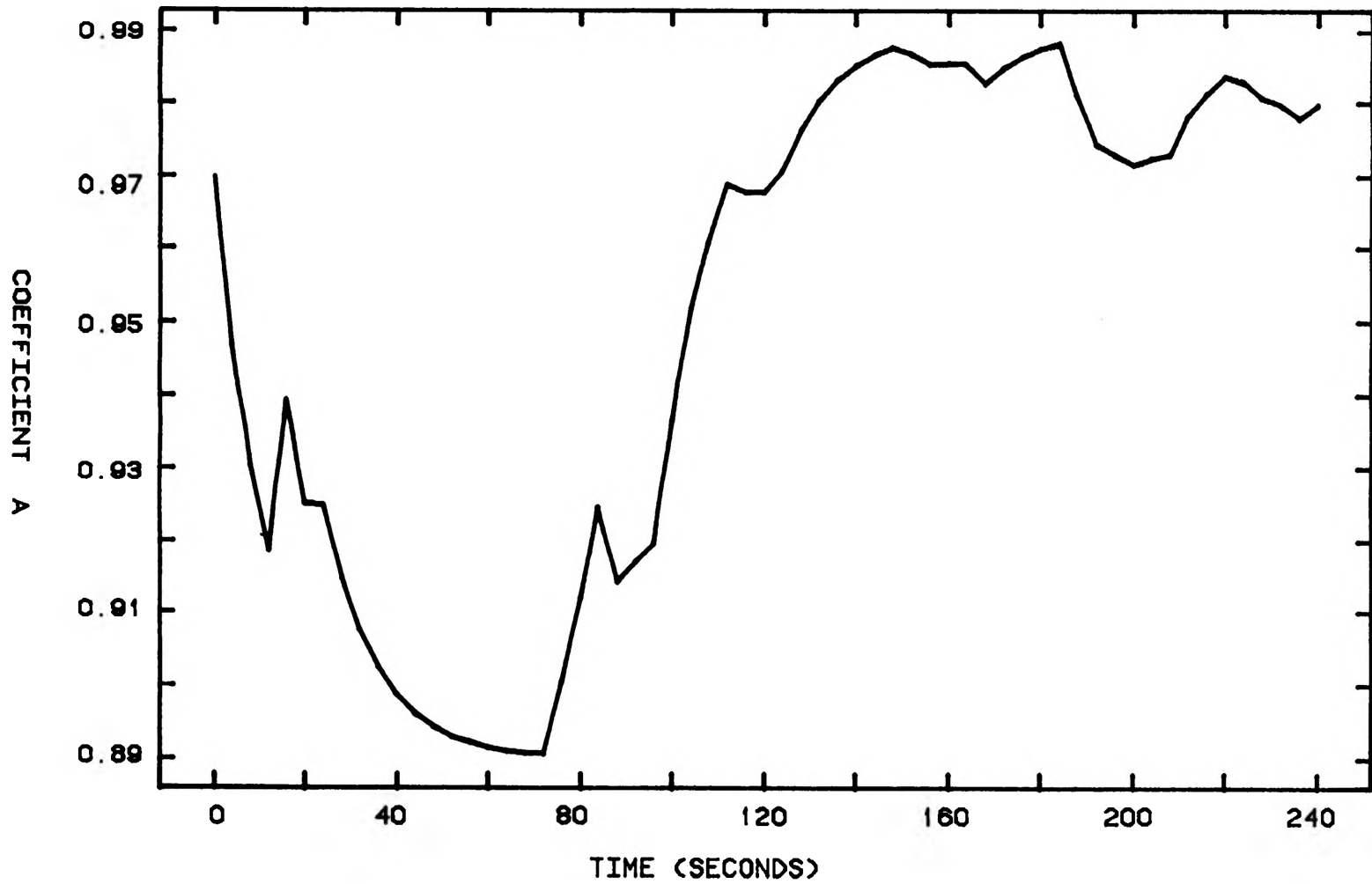


Figure 4.12. The coefficient A at the expansion rate of -0.0828 kPa/s or $-4^{\circ}\text{C}/\text{min}$.

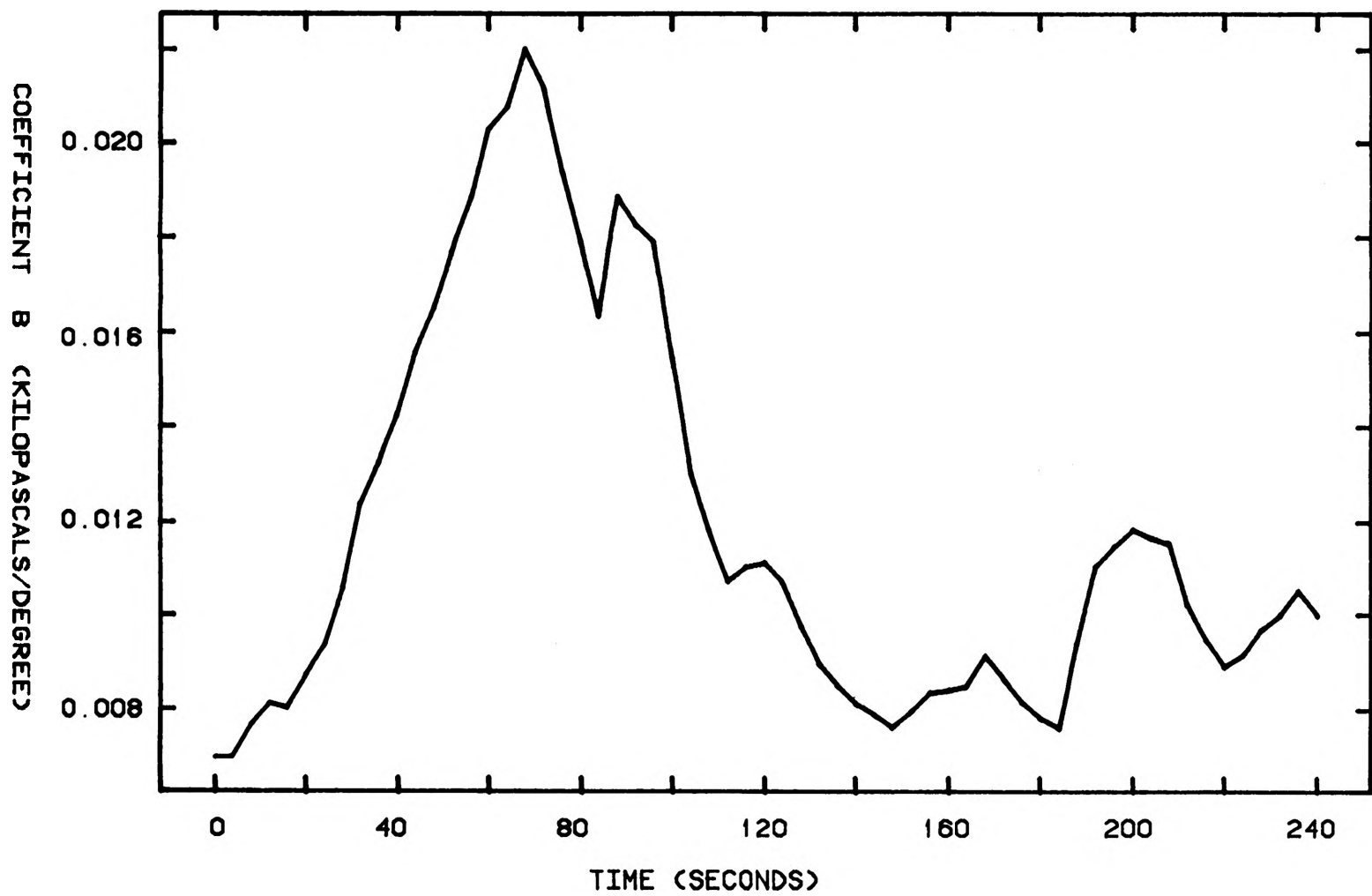


Figure 4.13. The coefficient B at the expansion rate of -0.0828 kPa/s or $-4^{\circ}\text{C}/\text{min}$.

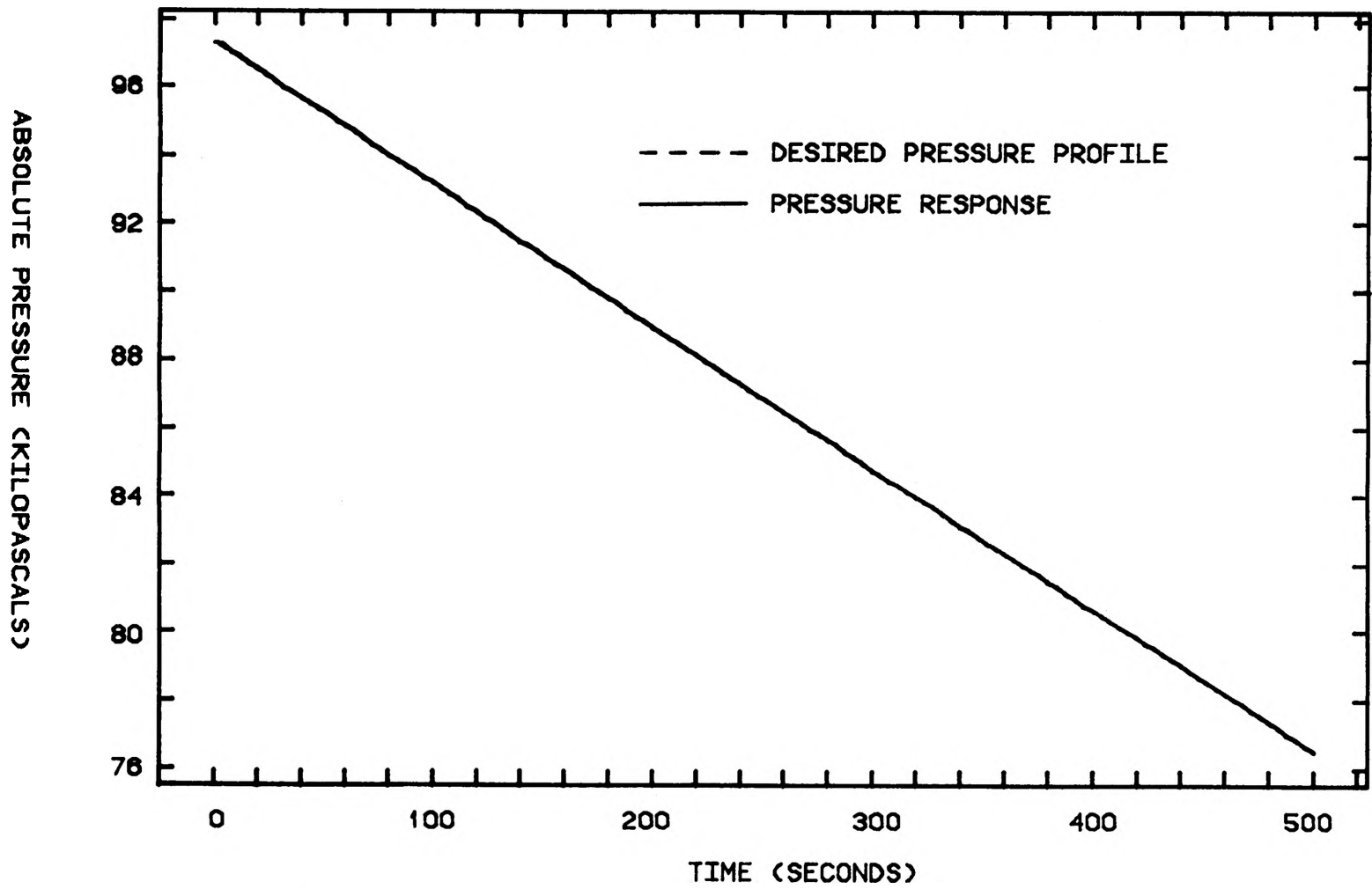


Figure 4.14. The pressure response at the expansion rate of -0.0414 kPa/s or $-2^{\circ}\text{C}/\text{min}$.

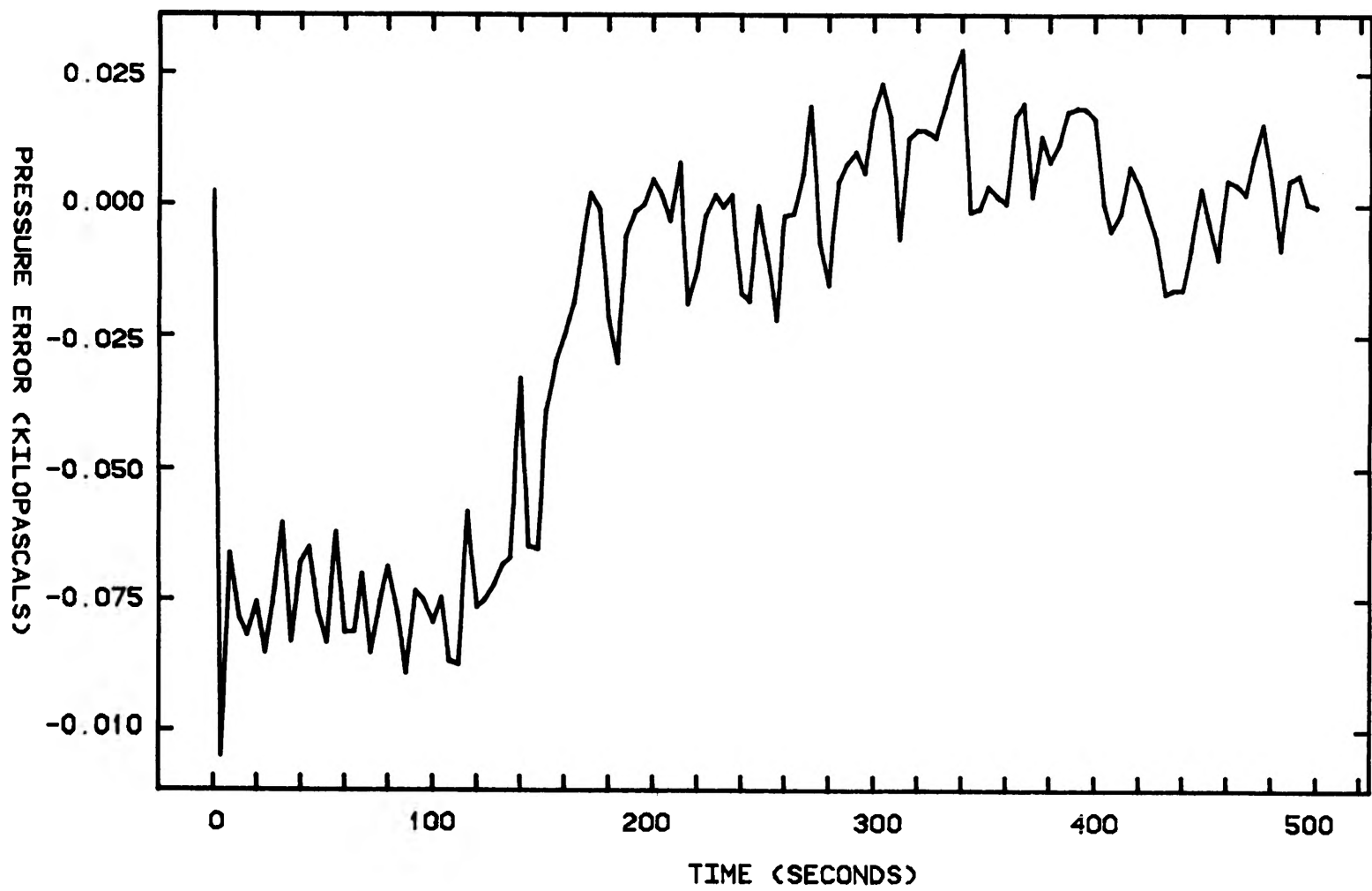


Figure 4.15. The pressure error at the expansion rate of -0.0414 kPa/s or $-2^{\circ}\text{C}/\text{min}$.

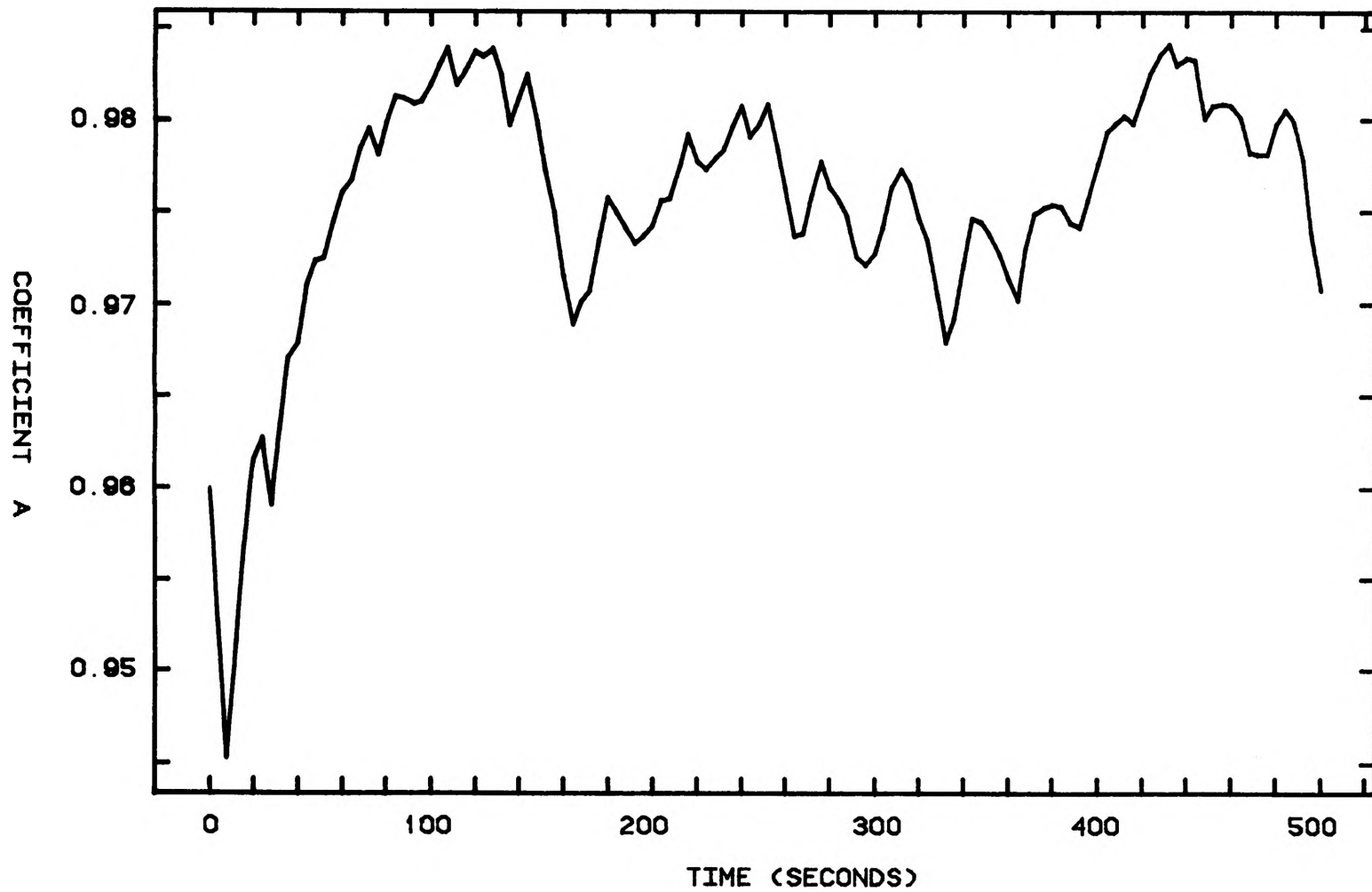


Figure 4.16. The coefficient A at the expansion rate of -0.0414 kPa/s or $-2^{\circ}\text{C}/\text{min}$.

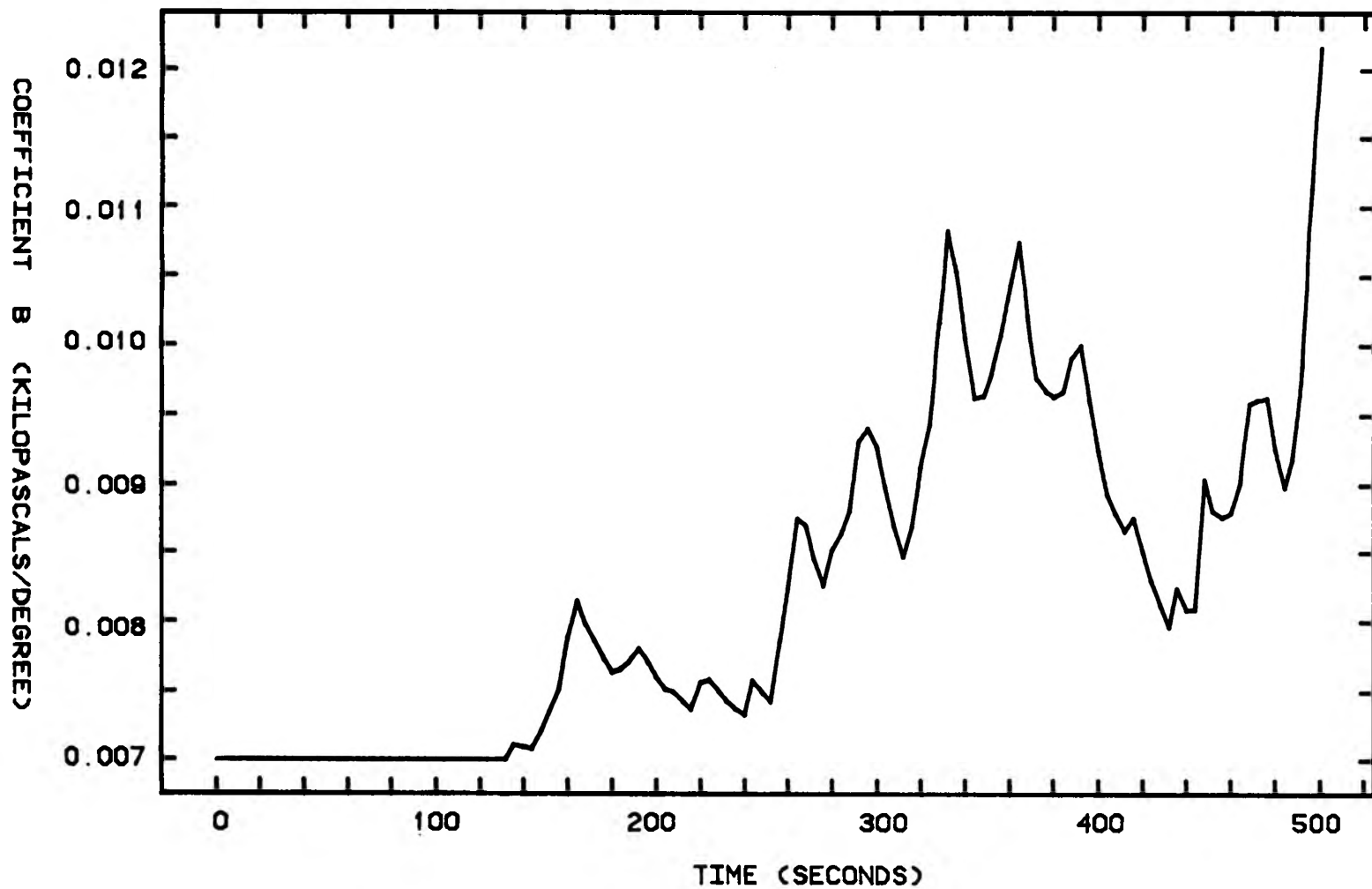


Figure 4.17. The coefficient B at the expansion rate of -0.0414 kPa/s or $-2^{\circ}\text{C}/\text{min}$.

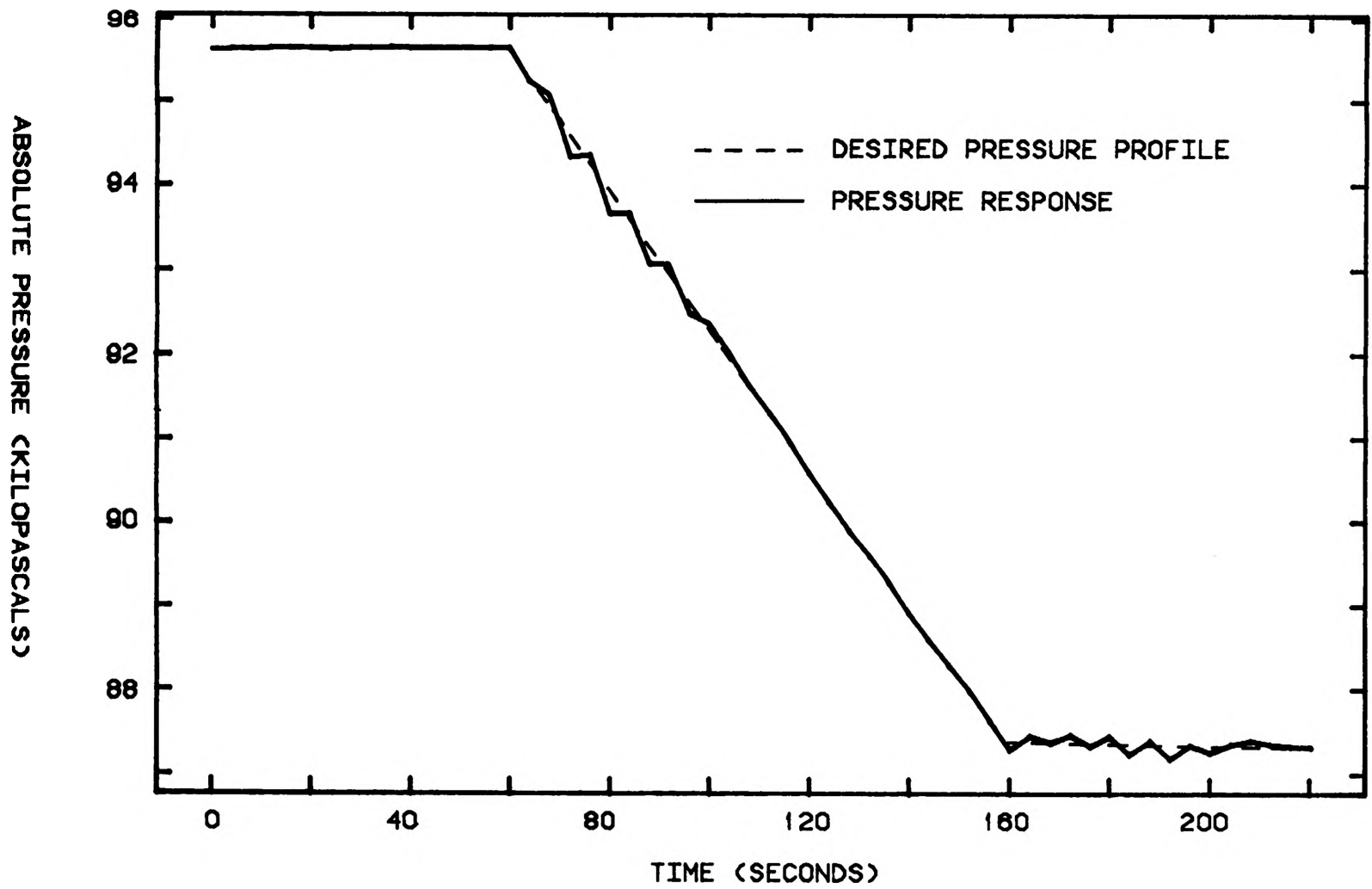


Figure 4.18. The pressure response including the holding modes.

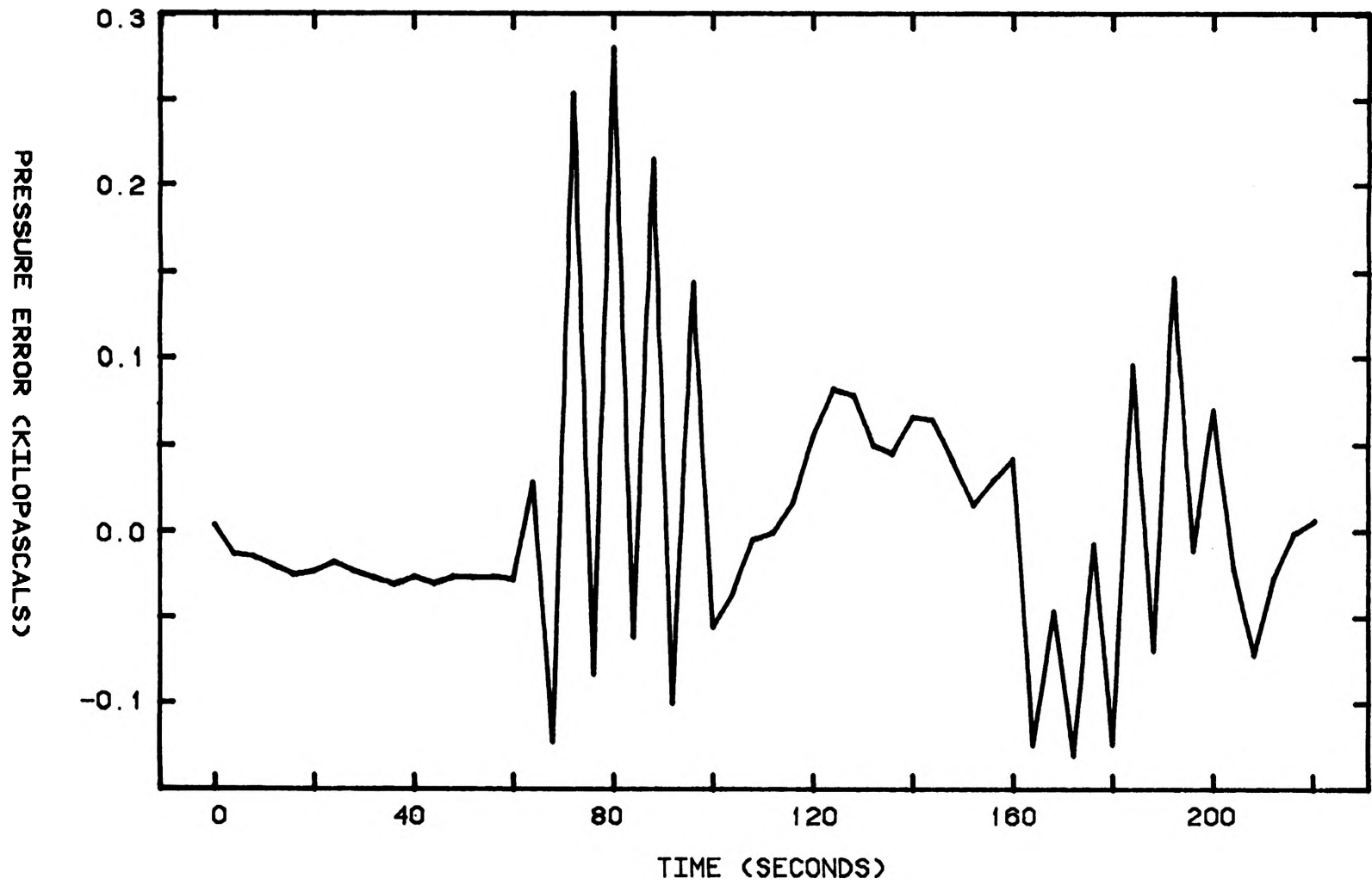


Figure 4.19. The pressure error including the holding modes.

holding time is 60 seconds. The result shows that the pressure response settles down within 60 seconds after the desired pressure profile changes slope.

V. CONCLUSION

The expansion system can be approximated by a first order quasi-linear model whose coefficients are A and B as shown in equation 3.5. A time-optimal control scheme using table look-up for the values of A and B was attempted. The attempt failed due to the fact that the range of validity of each table was very small. Thus, many tables were required and too much core memory was needed to store the tables on-line. Adaptive control using a sequential regression identification scheme eliminates the use of tables completely. But it still produces high rms error because the coefficients A and B belong to a system of the third type discussed in Section 3.D. The low pass digital filter and the constraint on the parameters ("flyability" [38]) introduced into the identification can reduce the rms error of the expansion system significantly. The closed-loop system is found to be stable and the parameters converge even though the initial values are off by 50%.

Based upon the experimental results, the following conclusions are reached:

1. The adaptive controller is capable of recovery from highly erroneous parameter estimates.
2. Control can be satisfactory even in the presence of parameter offset introduced by the low pass digital filter.

3. In view of computational requirements, the adaptive controller based upon the time-optimal control theory is implementable by the laboratory minicomputer, a NOVA 840.
4. Extension of the theories of linear systems to non-linear situations is quite successful in this case.
5. Use of a high level language, FORTRAN, again shows significant reduction of programming effort at the expense of small increases in computing time and memory.

This controller still has limitations. For example, it can control an expansion at the rate of -0.1242 kPa/s (-0.018 psi/s) or $-6^{\circ}\text{C}/\text{min}$ for only 18.6 kPa (2.7 psi) change in pressure because of limited pumping capacity. This problem can be eliminated by using a higher pumping capacity when the high rates of expansion are to be simulated.

The digital control of the expansion system described in this dissertation is presently in use with satisfactory results. Together with the wall temperature controller, the chamber is now operational over a much larger range of temperature and pressure change than before. Currently, about 15°C change in temperature and 20.7 kPa (3 psi) change in pressure can be controlled. This is about 10 times the range of operation of the analog controller

built by Tebelak [21]. The relative accuracy of the expansion controller, which is about 0.1% with respect to the total change of pressure, is slightly better than the relative accuracy, 0.13%, obtained from Tebelak's controller. The maximum rate of expansion is also increased to -0.1242 kPa/s (-0.018 psi/s) compared to -0.0104 kPa/s (-0.0015 psi/s) for Tebelak's controller.

It is also true that the adaptive controller exhibits an advantage over other control systems due to the fact that whenever a piece of hardware of the expansion system is updated, there will be either no change or a minor change in the software that controls that piece of hardware. In addition, the computer time required is only 8% of the total available time. This is a significant benefit, because the computation for the control does not load the computer. The computer time can be reduced to about 2% of time available by eliminating the minor loop for position control of the valve. This could be accomplished if a digital valve were used in place of the 3-way rotary valve.

The significant improvements in the quality of control mentioned above can not be accomplished without the implementation of the optimal control law and the use of the computer as an intelligent controller. It is hoped that this dissertation will serve as a reference for further development of the control systems of the cloud simulation chamber.

BIBLIOGRAPHY

1. Batten, Louis J., Cloud Physics and Cloud Seeding, 1st Ed., Anchor Books, New York, 1962.
2. Volkovitskii, O. A., Cloud Physics Experimental Investigations, Keter Publishing House Jerusalem Ltd., Jerusalem, 1974.
3. Perrie, D. W., Cloud Physics, John Wiley & Son, New York, 1950.
4. Kassner, J. L., Jr., J. C. Carstens, M. A. Vietti, A. H. Bierman, Paul C. P. Yue, L. B. Allen, M. R. Eastburn, D. D. Hoffman, H. A. Noble, and D. L. Packwood, "Expansion Cloud Chamber Technique for Absolute Aitken Nuclei Counting", Rolla: The University Press, 1967.
5. Aitken, J., Collected Scientific Papers of John Aitken, Cambridge Univ. Press, 1923
6. Report to McDonnell Douglas Astronautics Co., "Cloud Simulation Program", Graduate Center for Cloud Physics Research, University of Missouri-Rolla, Missouri, July, 1974.
7. White, D. R., D. E. Hagen, J. L. Kassner, Jr., D. R. Fannin, Paul Kriegshauser, and Alfred R. Hopkins, "A Thermoelectric Cooled Expansion Cloud Chamber", 2nd International Conference on Thermoelectric Energy Conversion, Arlington, Texas, March 22-24, 1978.

8. Hagen, Donald E., George M. Hale, and James M. Carter, "Laser Doppler Method for Cloud Droplet Size Spectrum" Graduate Center for Cloud Physics Research, Univ. of Missouri-Rolla, Missouri.
9. Kuo, B. C., Discrete-Data Control System, Science Tech, Champaign, Illinois, 1974.
10. Anderson, Brian D. O., and John B. Moore, Linear Optimal Control, 1st Edition, Prentice-Hall, N.J., 1971.
11. Report NAS8-31849-0003, Cloud Physics Laboratory Science Simulator, Third Quarterly Progress Report, Oct. 30, 1976 to Jan. 29, 1977, University of Missouri-Rolla, Missouri.
12. Podzimek, J., Fysike Oblaku (Cloud Physics), NCSAV, Praha, 1959, pp. 248.
13. Wilson, J. G., The Principles of Cloud-Chamber Techniques, Cambridge University Press, 1951.
14. Gunn, R., "The Electrification of Clouds and Raindrops", Atmosphere Explorations, H. G. Houghton, Editor (The Technology Press of M.I.T. and John Wiley, New York, 1958).
15. Podzimek, J., "A Study of the Formation of Ice Crystals in Low Pressure Chamber", Trans. Inst., Geophysics Techn. Acad. Sci, No. 213, Geofysikalni Sbornik, 1964.

16. Volkovitskii, O. A., "A Complex of Experimental Installations for Geophysical Investigations", *Meteorologiya i gidrologiya*, No. 6 (in Russian), 1955.
17. Edwards, G. R. and L. F. Evans, "Ice Nucleation by Silver Iodide: II Collision Efficiency in Natural Clouds", *J. Meteor.*, Dec, 1961.
18. Steele, R. L. and F. W. Smith, "Experimental Facility for Simulation of Adiabatic Cloud Processes", Proceedings, First National Conference on Weather Modification, Albany, New York, April 28 - May 1, 1968.
19. Oetting, R. B., J. L. Kassner, Jr., and T. L. Holeman, "Design and Development of a New Type Cloud Simulation Chamber", Paper presented at Meeting of American Geophysical Union, San Francisco, California, Dec 15-18, 1969.
20. Tebelak, A. C., "Design of an Analog-Temperature Control System for an Expansion Cloud Chamber", M.S. Thesis, University of Missouri-Rolla, Missouri 1973.
21. Hagen, D. E., A. C. Tebelak, and J. L. Kassner, Jr., "A Cloud Chamber Control System", *Rev. Sci. Instrum.*, Vol. 45, No. 2, February 1974.
22. The Expansion Control System User's Manual, Graduate Center for Cloud Physics Research, University of Missouri-Rolla, Missouri, 1978.
23. Cutler, H., "Linear Velocity Ramp Speeds Stepper and Servo Positioning", *Control Engineering*, May, 1978.

24. The Expansion Control System Software Manual, Graduate Center for Cloud Physics Research, University of Missouri-Rolla, Missouri, 1978.
25. Takahashi, Yasundo, Michael J. Rabins, and David M. Auslander, Control and Dynamic Systems, 2nd E., Addison-Wesley Publishing Company, 1972.
26. Lee, T. H., G. E. Adams, and W. M. Gaines, Computer Process Control Modeling and Optimization, John Wiley & Son, New York, 1968.
27. Warner, D. E. and E. Dawson Ward, "Filter Sequential Regression Parameter Identification Applied to a Gas Turbine Engine Model", Journal of Dynamic Systems, Measurement and Control, Trans. ASME, Series G, Vol. 99, No. 4, December, 1977.
28. Salahi, Javad, "System Transfer Function Identification by Gradient Techniques", M.S. Thesis, University of Missouri-Rolla, Missouri, 1976.
29. Widnall, William S., "Applications of Optimal Control Theory to Computer Controller Design", Research Monograph No. 48, The M.I.T. Press, Cambridge, Massachusetts, 1968.
30. Athens, Michael, Michael L. Dertouzos, Richard N. Spann, and Samuel J. Mason, Systems, Networks, and Computation: Multivariable Methods, McGraw-Hill, 1974.
31. Mini-issue on NASA's Advanced Control Law Program for the F-8 DFBW Aircraft, IEEE Trans. Auto. Control, Vol. AC-22, No. 5, October, 1977.

32. Rault, A., J. Richalet, A. Barbot, and J. P. Sergenton, "Identification and Modelling of a Jet Engine", IFAC Symposium on Digital Simulation of Continuous Processes, Győr, Hungary, 1971
33. Kohr, R. H., "On the Identification of Linear and Non-Linear Systems", Simulation, March, 1967.
34. Ward, E. D., "Identification of Parameters in Non-linear Boundary Conditions of Distributed Systems with Linear Fields", Journal of Dynamic Systems, Measurement and Control, Trans. ASME, Series G, Vol. 95, No. 4, December 1973.
35. Ward, E. D., and R. G. Leonard, "Automatic Parameter Identification Applied to Railroad Car Dynamic Draft Gear Model", Journal of Dynamic Systems, Measurement and Control, Trans. ASME, Series G, Vol. 96, No. 4, December, 1974.
36. Weinberg, M. S., and G. R. Adama, "Low Order Linearized Model of Turbine Engines", Report Number ASK-TR-75-24, Air Force Systems Command-Aeronautical Systems Division, Wright-Patterson Air Force Base, Ohio, July, 1975.
37. System Reference Manual, "Fortran IV User's Manual, 093-000053-06", Sixth Revision, Data General Corporation, 1973.
38. Cicolani, L. S., and George Meyer, "Digital Simulation of V/STOL Aircraft for Autopilot Research", Large Scale Dynamic Systems, NASA SP-371, 1975.

VITA

Katiya Greigarn was born on June 10, 1952, in Samutprakan, Thailand. He received his elementary education at various schools in Bangkok, and was graduated from Tram Udom Suksa High School in Bangkok, Thailand in March, 1969. He received his college education from Chulalongkorn University, Bangkok, where he received his Bachelor of Electrical Engineering degree in June, 1973. He enrolled in the Graduate School of the University of Missouri-Rolla in January 1974. He has worked as a graduate research assistant in the Cloud Physics Research Center since August 1975. He received his Master of Science Degree in Electrical Engineering at the University of Missouri-Rolla in July 1976.

He is a member of the Engineering Association of Thailand and the Institute of Electrical and Electronics Engineers in the United States. Currently, he is the president of the Thai Student Association of the University of Missouri-Rolla.